UNIVERSITA' POLITECNICA DELLE MARCHE

FACOLTA' DI **INGEGNNERIA**

Corso di Laurea magistrale in **Environmental Engineering**

Pseudo constant tracer release as a cost-effective tracer test technique to characterize groundwater travel times

Relatore:

Dott. **Nicolò Colombani**

Tesi di Laurea di:

Sher Shah

A.A. **2021/2022**

Acknowledgments

From the depth my heart, I want to thank my supervisor Prof. Nicolò Colombani, who guided me and supported me during my whole research work.

Special thanks to the PhD students Luigi Alessandrino and Mattia Gaiolini, for their kindness and the support they provided me in the laboratory experiments.

Moreover, I would like to express my sincere thanks to all the faculty members of Department of Environmental engineering.

Particularly, I want to acknowledge support, efforts and prayers of my parents, and siblings, and the motivation from Elisa Blumenthal, which has directly been encouraging me for my studies.

Table of Contents

Introduction **1**

1. Groundwater: definition and importance **2**

1.1 Definition of groundwater 2

1.2 The value and the problems of groundwater 3

1.3 Groundwater – surface water interaction 5

1.3.1 Heat tracer methods 6

1.3.2 Methods based on Darcy's Law 6

1.3.3 Mass balance approaches 9

1.4 Methods for determining the concentration of contaminants 9

2. Tracer techniques **10**

2.1 History of tracers 10

2.2 Types of tracers 11

2.2.1 Artificial tracers 11

2.2.2 Environmental tracers 12

2.3 Tracer test methods 12

2.3.1 Natural gradient tracers (NGTT) 14

2.3.2 Force gradient tracer test (FGTT) 14

2.3.3 Multi-tracer approach and DNA sequence-based tracers 15

3 Material and Methods **17**

3.1 Laboratory Instruments 17

3.1.1 Design of Tank 17

3.1.2 Wells and piezometers 18

3.1.3 Data loggers and monitoring probes 19

3.1.4 Physical parameters and hydraulic properties 21

3.1.5 Biodegradable plastic bags (PLA) 23

3.1.6 Other Instruments used 26

3.2 Experiments 27

3.2.2 Column experiment (With different flows) 28

3.2.3 Tank Experiments 28

4 Results and discussion **30**

4.1 Batch experiment (no flow conditions) 30

4.2 Column experiment 32

4.3 Tank experiment 36

4.3.1 Tank experiment without osmotic exchange bags 36

4.3.2 Tank experiment with PLA osmotic exchange bags 43
4.3.3 Tank experiment with PLA osmotic exchange bags in a single well 47
Conclusions **51**
References **53**

List of figures

Figure 1. 1: Zones of aeration and saturation (Prasad, 2002). 2
Figure 1. 2: Types of aquifers (Prasad, 2002). 3
Figure 1. 3: Functions and services offered by groundwater systems (der Gun, 2021). 4
Figure 2. 1: Approaches for using tracer test-based data (Ptak et al., 2004) 13

Figure 3. 1: 3D tank in hydrogeological laboratory, SIMAU, 18
Figure 3. 2: HDPE tubes around the monitoring wells 19
Figure 3. 3: (a) Soil & Water Diver water level data-logger, (b) Em 50 data logger (Decagon devices) 20
Figure 3. 4: Column of sieves placed in a mechanical shaker. 23
Figure 3. 5: Life cycle of PLA. 24
Figure 3. 6: Methods for PLA production. 24
Figure 3. 7: PLA biodegradable plastic bag as an exchange membrane for NaCl Salt. 25
Figure 3. 8: (a) Data logger used in outlet of the tank, (b) Peristatic pump (MINIPULS® 3 Gilson) 26
Figure 3. 9: BARO-Diver for recording the atmospheric pressure 26
Figure 3. 10: Flow diagram of the laboratory experiments performed. 27
Figure 3. 11: 1-D experimental setup and apparatus 28
Figure 3. 12: Single monitoring well test for checking the vertical flow velocity. 29
Figure 4. 1: Time variation of electrical conductivity. 31
Figure 4. 2: Time variation of electrical conductivity with flowrate of 18 mL/min. 32
Figure 4. 3: Time variation of electrical conductivity with flowrate of 10 mL/min 33
Figure 4. 4: Time variation of electrical conductivity with the flowrate of 3 mL/min. 34
Figure 4. 5: Mass loading rate versus specific discharge. 35
Figure 4. 6: Water level for the points A2, B2, C2 and D2. 36
Figure 4. 7: Observed temperatures in each monitoring point versus time. 39
Figure 4. 8: Observed electrical conductivity in each monitoring point versus time 41
Figure 4. 9: Water level for the points A2, B2, C2 and D2. 44
Figure 4. 10: Observed EC in each monitoring point versus time 45
Figure 4. 11: Depth of the water recorded by the probes with variation of time. 47
Figure 4. 12: Time variation of EC in a single monitoring well, note that Port 4 has a secondary Y axis (on the right). 48
Figure 4. 13: Comparison of EC between the MLS outside D2 and in monitoring well D2. 50

List of tables

Table 3. 1: Horizontal distance of probes from each other. 18
Table 3. 2: meter group ECH20 5TE soil moisture sensor features 21
Table 3. 3: Parameters of sediments and their standard deviation. 23
Table 3. 4: Physical and mechanical properties of PLA. 25
Table 4. 1: Time variation of EC through the diffusion from PLA bag. 30
Table 4. 2: Calculation of specific discharge. 35
Table 4. 3: Hydraulic gradient between the monitoring wells. 37
Table 4. 4: Velocities calculated from Darcy Law. 38
Table 4. 5: Average velocity measured from different measuring points taken at the (temperature (inflection point). 40
Table 4. 6: Average velocity calculated from the inflection points and peak of Gaussian BTC of EC among monitored points. 41
Table 4. 7: Retardation factor calculated by velocity from EC over velocity from temperature. 43
Table 4. 8: Average velocity calculated from the inflection points of EC among the monitored points. 45
Table 4. 9: Hydraulic gradient between monitoring wells. 46
Table 4. 10: Calculated Darcy's and seepage velocities. 46
Table 4. 12: Calculation of the average velocity of the flow from the time taken to achieve breakthrough curves. 49
Table 4. 13: EC values obtained from actual aquifers in the tank 49

Introduction

Groundwater is a natural resource with inestimable value. Its importance is not only given by the fact that it represents a source of water for human needs, but it also offers various other services such as supporting and regulatory ones, like feeding groundwater dependent ecosystems (Eamus et al., 2015; Kløve et al., 2011). However, in the last years groundwater resources have been exposed to immense stress such as intensive abstraction, salinization, and pollution, compromising the possibility to be used for certain scopes (van der Gun, 2021). Due to its importance, research activities are carried out to find the contamination as early as possible, and the remediation of groundwater.

In hydrogeology, tracer techniques are used to estimate the effective parameters for describing reactive and non-reactive transport process in an aquifer or in laboratory experiments and can range from dissolved species found or injected in groundwater or a water property used for the interpretation of the environmental processes (Ptak & Teutsch, 1994). Tracers have been used for centuries and the advancement in the techniques and materials used are increasing with the development of the research activities.

To characterize the subsurface properties and to examine the spreading of both non-reactive and reactive solutes in groundwater, these techniques are found to be very effective. The use of sodium chloride salt is used as conventional tracing technique. These techniques are limited by a number of issues due to non-ideal behavior of sodium that may undergo cation exchange and the change in density and viscosity of the fluids due to elevated concentrations that may develop in groundwater due to high salt solubility. To overcome the latter issue, ion exchange membranes could be employed to slowly release the tracer in solution since they avoid concentrations spikes (Garcia-Vasquez et al., 2014), but are very costly and this may limit their wide use especially in developing countries.

Within this framework, this thesis work analyzed a cost-effective replacement of the osmotic exchange membranes with low cost Polylactide (PLA) bags and continuous monitoring via low-cost probes to avoid time consuming field sampling and costly laboratory analyses thus providing a cost-effective tracer test technique feasible also for limited budget situations. The laboratory experiments were performed in SIMAU department of Università Politecnica delle Marche.

Chapter 1 discusses the values and problem associated to groundwater resources and its interactions with the surface water. Chapter 2 explains the history of tracers, techniques of tracers and their limitations. Chapter 3 describes the material and methods used for the experimental activities. Chapter 4 presents and discusses the obtained result

1. Groundwater: definition and importance

1.1 Definition of groundwater

Groundwater is one of the main natural resources and, if well managed, it can contribute to a sustainable development which can meet the needs of the present water demand without compromising the possibility for the future generations (der Gun, 2021). It consists of the portion of water which fill the porous spaces of the soil, sediments, and rocks beneath the earth surface until reaching an impermeable layer. Groundwater can be collected with wells, drainage galleries or tunnels, and it is better distributed than the surface water. The bodies of rocks and sediments which contained the groundwater are called aquifers. Groundwater can be recharged by precipitation and snowmelt, but also from other sources including irrigation and leaks from water supply systems. The recharge can be accomplished via infiltration or percolation. Infiltration consists of the movement of water downward into the soil and percolation is the vertical and lateral motion of water due to gravity or pressure through the openings in geological material. Below the earth's surface it is possible to identify a zone of aeration and a zone of saturation. The zone of aeration is the area between the soil surface and the water table. The water of this zone is defined as capillary water. The zone of saturation is the one filled with water under hydrostatic pressure (fig. 1.1) (National Geography Society, 2022; Prasad, 2002).

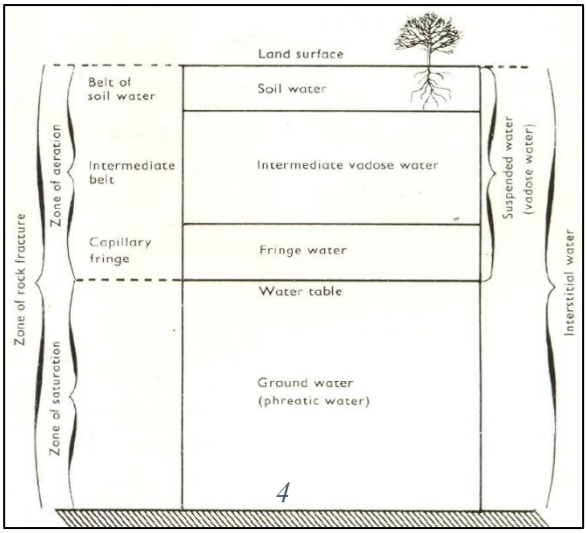

Figure 1. 1: Zones of aeration and saturation (Prasad, 2002).

According to the hydrogeologic classification, the rocks can be classified as aquifers, aquitards, aquicludes and aquifuges. Aquifers occur when the formation is sufficiently permeable (e.g., sand and gravel deposits). Aquicludes are impermeable formations (e.g., clay beds). Aquitards

consist of formations which are less permeable than aquifers but not impermeable (e.g., sandy clay). Aquifuges are the formation which neither hold nor transmit groundwater (e.g., massive hard rocks). Aquifers can be classified as unconfined, semi-confined and confined. In unconfined aquifers the surface of groundwater body is at atmospheric pressure. These aquifers are also called "phreatic aquifers". The semi-confined aquifers are the ones bounded by one or two aquitards. The confined aquifers are the ones between two impermeable layers. In the later one, the pressure condition is characterized by the piezometric surface: when it is above the soil surface, the well is called "artesian well" (fig. 1.2) (Prasad, 2002).

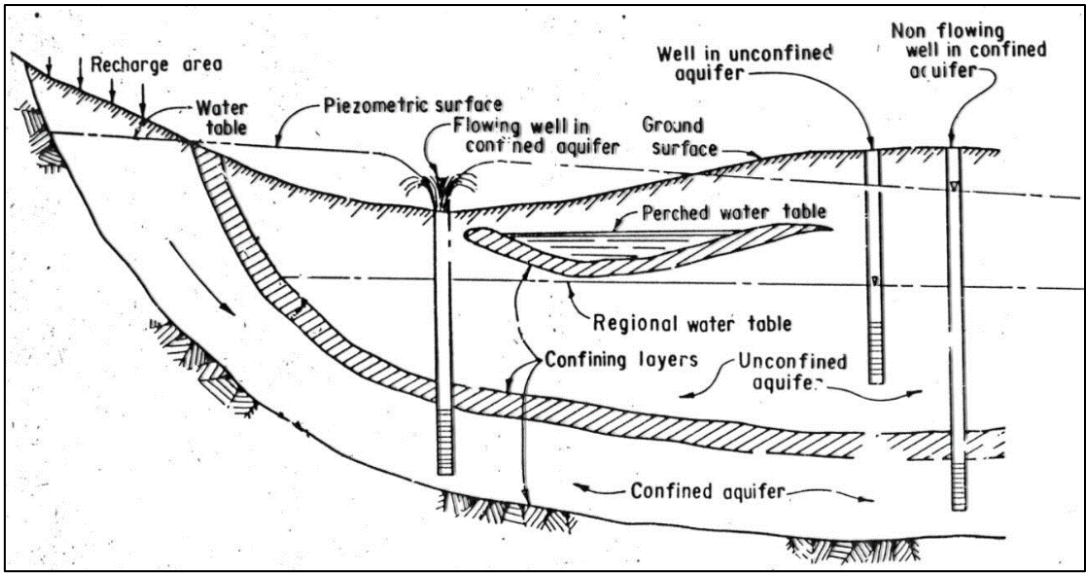

Figure 1. 2: Types of aquifers (Prasad, 2002).

1.2 The value and the problems of groundwater

Groundwater is a precious resource not only limited as being a source of water for human needs (it provides almost half of all drinking water worldwide), but it can have different functions providing numerous services as it is shown in fig. 1.3 (der Gun, 2021; NGWA, 2022).

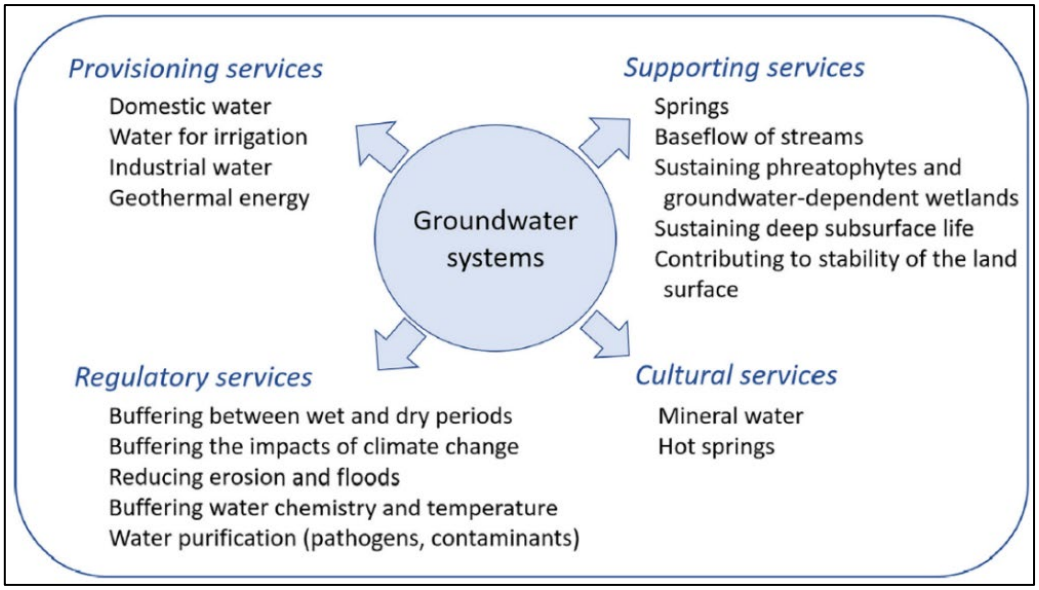

Figure 1. 3: Functions and services offered by groundwater systems (der Gun, 2021).

Groundwater can be considered a sustainable resource, as long as it is able to provide essential services. This year, the groundwater was the main character of the world water day titled as "groundwater – making the invisible visible", to highlight its inestimable value. Moreover, the sixth sustainable development goal of Agenda 2030 is to "ensure availability and sustainable management of water and sanitation for all", including among the six "outcome-oriented targets" the protection and remediation of water-related ecosystems.

However, recently groundwater resources have been exposed to immense stress such as intensive abstraction, artificial drainage, salinization, pollution, climate change and sea-level rise (der Gun, 2021).

Its withdrawal rates are currently estimated in the range of 982 km^3/year (NGWA, 2022). In 2018 it was reported that the withdrawals of groundwaters due to irrigation in agriculture were around 820 km^3/year and it increased comparing to 2010 (FAO, 2021). The intensive abstraction and the artificial drainage can cause, among the other, land subsidence, saline intrusion, and low-quality water (der Gun, 2021).

The agriculture is considered the major source of water pollution in many countries. The use of nitrogen synthetic fertilizer has increased, starting from almost 81 million tons in 2000 to 110 million tons in 2017, followed by a slight decline in 2018. The use of phosphorus started with 32 million tons in 2000 and reached 45 million tons in 2016, then it followed a marked decline (FAO, 2021). Nitrogen and phosphorus are essential nutrients for plants and animals, but their overabundance in water can be responsible of health and ecological issues (USGS, 2018). A high presence of nitrogen and phosphorus in water bodies causes the phenomenon

known as eutrophication: the overabundance of nutrients causes the growth of algae which, once they end their life cycle, are decomposed by bacteria. This process consumes oxygen and can lead to hypoxic environments, causing the death of life species like fishes (USGS, 2019). Consuming water with high nitrogen content can cause methemoglobinemia in infants under six months of age, but also other severe problems such as cancer and birth defects (Ward et al., 2018).

Another major threat for drinking purposes of groundwater is its salinization. Saline groundwater can be generated by different causes including anthropogenic pollutants such as fertilizers. If salinized water is used for irrigation, it can reduce crop yields or make the land unsuitable for further agricultural purposes (Cuevas et al., 2019; Rhoades et al., 1992). The consumption of water which contain an excess of salt by human can lead to conditions of hypertension (van Weert et al., 2009). Once water become salinized or polluted, it cannot be use for certain services, like for domestic water supply.

Regarding climate changes, numerous studies showed that they cause the increase of average temperature and sea-level. Higher temperatures are usually responsible of diminishing groundwater recharge, increased evapotranspiration rates and the sea-level rise contribute to saline intrusion especially in the Mediterranean area (Mastrocicco & Colombani, 2021).

1.3 Groundwater – surface water interaction

The exchange processes and pathways between groundwater and surface water are of fundamental importance for the protection of water resources. Understanding the mass flowrate between groundwater and surface water is crucial in case of contamination. The interaction between groundwater and surface water occurs when the groundwater is alimenting the stream (gaining stream) and when, conversely, the stream is infiltrating through the sediments until it reaches groundwater (losing stream). The happening of one or the other depends on the hydraulic head: when the elevation of the groundwater table is more than the stream one there will be a gaining reach, while the opposite will lead to a losing reach. Precipitation events or seasonal variations can be responsible of changing the direction of exchange flow. The estimation of the quantity of water exchanged between groundwater and surface water is challenging due to heterogeneities and the needing to integrate measurement at different scales (Kalbus et al., 2006).

Among the approaches used for studying the interaction between groundwater and surface water there are the heat tracer methods, the methods based on Darcy's Law and the ones which consider the mass balance.

1.3.1 Heat tracer methods

Surface water and groundwater have different chemical, biological and physical properties. For this reason, the different temperatures which characterize these two water bodies can be used for estimating the discharge or recharge between them. Groundwater temperatures stay stable during the year while the ones of surface water have great variability based on the daytime and the season. In this sense, the gaining reaches are recognized by the stability of temperature while the losing reaches by the highly variable temperatures. The transport of the heat in the sub-surface is a result of the combination of advective heat transport and conductive heat transport and it can be described through a heat transport equation for which different analytical and numerical solution have been developed, allowing the calculation of the seepage rates starting from the temperature profiles. Moreover, streambed temperatures are very sensitive to hydraulic conditions. Considering this, measurement of the streambed at various location should be done in a short period of time, associating the different temperature values to the spatial variation of water flux through the streambed. The measurement of the temperature can be considered cheap, quick, and easy to perform (Kalbus et al., 2006).

1.3.2 Methods based on Darcy's Law

The methods based on Darcy's Law are usually applied for the study of groundwater movement in terrestrial aquifers and require finding the components of the Darcy equation:

$$q = -K\frac{dh}{dl}$$

Where:
q – specific discharge [L/T]
K – hydraulic conductivity [L/T]
h – hydraulic head [L]
l – distance [L]

The specific discharge (Darcy velocity) can be observed using tracer methods and considering the porosity:

$$v = \frac{q}{n}$$

Where:
v – water velocity [L/T]
q – Darcy flux [L/T]
n – porosity [-]

For determining the water flux in the subsurface, hydraulic gradient and hydraulic conductivity or groundwater velocity and porosity are usually needed (Kalbus et al., 2006).

The hydraulic head can be determined by measuring the water level in wells and piezometers. Different hydraulic heads of a group of piezometers allow to determine the direction groundwater flow of a specific area. This method is easy and lead to a detailed survey of the heterogeneity of flow conditions. However, it must be considered that the movements of groundwater are subjected to temporal variations and consequently the resulting flow field maps are representative just of a specific time (Kalbus et al., 2006).
Hydraulic conductivity can be estimated starting from the grain size, through permeameter tests, with slug and bail tests and with pumping tests.
Considering the grain distribution of a sediment sample, the hydraulic conductivity can be estimated through empirical relations between statistical parameters of the grain size and the hydraulic conductivity. The value of hydraulic conductivity founded in this way can be used as a first estimation for designing further applications such as slug and bail tests.
The permeameter tests are performed in laboratory enclosing a sediment sample between two porous plates in a tube. For a constant-head test, the hydraulic conductivity can be calculated from Darcy's law. In a falling-head test the hydraulic conductivity can be calculated from the head difference, the time, and the geometry of the tube and the sample. It must be considered that it is difficult to maintain the packing and the orientation of the sediment grains during sampling and transportation, and this can change the results. For measuring the vertical hydraulic conductivity of the streambed, an in situ permeameter test using a standpipe pressed into the sediment can be applied. The pipe is filled with water and the level fall is recorded.

Hydraulic conductivity can be calculated starting from the difference in hydraulic head, in time and the length of the sediment column. Alternatively, the level of water in the pipe can be healed constant and the injection rate is used for the analysis. The horizontal hydraulic conductivity can be achieved with a constant-head injection of water in a screened piezometer. The permeameter tests performed in situ are quick and easy and give point measurement of hydraulic conductivity of the streambed (Kalbus et al., 2006).

Slug and bail tests consist of introducing or removing a known amount of water in or from a well or piezometer, measuring the head as a function of time, as the water level recover. These tests are quick and easy and use inexpensive equipment. These methods are indicated for analyzing heterogeneities providing point measurements of hydraulic conductivities.

The application of pumping test for determining the hydraulic conductivity needs the existence of a well for pumping water at a constant rate and a piezometer for recording the drawdown as a function of time. There are several methods for determining the hydraulic properties of the subsurface starting from these tests. However, the boundary conditions represent a problem for estimating the hydraulic conductivities of the streambed for the analysis of the interaction between the groundwater and the surface. The values of hydraulic conductivity achieved with pumping tests are representative for the entire subsurface body representing a large sub-surface volume. It must be considered that the cost of piezometer is high, and their application is not always possible (Kalbus et al., 2006).

The measurement of the hydraulic head, the analysis of the grain size and the permeameter test consist of point measurements. Slug, bail, and tracer tests give information in the scale of meters around the point of sampling. Among the methods applied in the subsurface, pumping tests operate on the largest scale (tens of meters up to kilometers). Grab sampling and passive samplers give point measurement of the contaminant concentration while integral pumping tests provide a concentration averaged over a large scale of volume subsurface (Kalbus et al., 2006).

The groundwater velocity can be determined using a conservative tracer like a salt like calcium chloride, introducing it in a well and recording its travel time for arriving at a downstream observation well. Since the groundwater has low velocities, the wells should be close enough for allowing to obtain the velocity results in reasonable time. For these reasons, only a small portion of the subsurface can be studied with this method, and the flow direction must be previously known. Alternatively, a dye tracer can be added, and its concentration continuously measured, deriving the groundwater velocity from the tracer dilution curve (Kalbus et al., 2006).

1.3.3 Mass balance approaches

The mass balance approach assumes that any gain or loss of surface water or any change in sub-surface water properties can be related to the water sources.

The hydrograph separation using the isotopic and geochemical tracers allows to achieve information on temporal and spatial origin of the components of the streamflow. In order to recognize a rainfall event or a pre-event flow, stable isotopic tracers can be applied because usually the isotopic composition of the rain is different than the one of the waters already in the catchment. Geochemical tracer and trace elements are usually applied for determining the fraction of water which is flowing along different subsurface paths. The main drawbacks of the trace-based hydrograph separation methods are the possible similarity of the isotopic composition of pre-event and event waters and the fact that the composition is not usually constant in space and time (Kalbus et al., 2006).

The solute tracers can be used for analyzing the interaction between the interstitial and the stream water in the sediments of the streambed. The temporary detainment of stream water (transient storage) is studied by injecting a conservative tracer into the stream and analyzing the tracer breakthrough curves for determining the size and the exchange rate of the zone (Kalbus et al., 2006).

1.4 Methods for determining the concentration of contaminants

The measurement of the concentration of contaminants can be done using monitoring wells, passive and grab samplers. Piezometers or monitoring wells allow the collection of samples of subsurface water. With a dense grid of multi-level samplers monitoring wells, it is possible to achieve a very detailed knowledge about the contamination (Sudiky, 1986). However, the study with the monitoring wells is difficult to apply in very large sites because of maintenance costs and time required to sample large amount of multi-port wells. The accumulation of contaminants with passive samplers is achieved via diffusion and/or sorption over long period of time. Once being sampled, the contaminants are removed with solvent extraction or via thermal desorption before being chemically analyzed. This method is time and cost efficient for long term application and allows to detect even very low contaminant concentrations and volatile organic compounds.

The concentration of the contaminant in the surface water can be estimated analyzing the water from grab or bottle samples. Among the drawbacks of this method there is the need of large volume samples for trace levels contaminants (Kalbus et al., 2006).

2. Tracer techniques

In hydrogeology, tracer techniques are used to estimate the effective parameters for describing reactive and non-reactive transport process in an aquifer or in a laboratory experiment (Ptak et al., 2004). Any material found in water or a water property that can be measured and used to interpret environmental processes is referred to as a "tracer" in hydrogeology (Cook, 2015). Tracing methods are widely used in science and have proven particularly beneficial in hydrogeology (Divine & McDonnell, 2005).Tracer can be artificial or environmental, an artificial tracer can be injected intentionally to know the purposes while environmental tracers are found naturally in groundwater or produced by through human activities intentionally or accidentally (Cook, 2015; Divine & McDonnell, 2005). To characterize the subsurface properties and to examine the spreading of both non-reactive and reactive solutes in groundwater, these techniques are found to be very effective. It can be performed at different scales of investigation, at laboratory scale and at field scale in kilometres (Ptak et al., 2004).

2.1 History of tracers

Since ancient times, applied tracers have been extensively utilized to determined groundwater velocities and characterize flow paths. Approximately in 10 A.D. a Jewish historian Flavius Josephus documented of finding link between the spring of Jordan river and a nearby pond using chaff as a tracer (Divine & McDonnell, 2005). Probably the first environmental tracers were used by the Greek through the karst system by transportation of small animals and objects. They used to throw objects in the springs for the verification of environmental tracers' observation (Cook, 2015). In the late 19th century, uranine dye was used as artificial tracers (Cook, 2015) and chloride, fluorescein and bacteria were used for the first time as quantitative tracers in the Europe (Divine & McDonnell, 2005).

Following World War II, the quantification of low tracer breakthrough concentration and high frequency sampling become feasible due to advancement in the analytical chemistry and sampling technologies, which also increased the use of different materials as tracers (Divine & McDonnell, 2005). To understand the groundwater recharge and the flow paths of the rainfall, applied tracers were used in 1960's (Divine & McDonnell, 2005). From 1960's to the 1980's isotopic methods were mainly used in the research of environmental tracers (Cook, 2015) since they are virtually lacking the problems of flow field perturbation during the tracer injection and namely behave as water molecules. To better understand the solute transport phenomenon in the porous medium, applied tracers have been used for the past 30 years (Divine & McDonnell,

2005). In 1980's, for comparing observed field-scale solute dispersion and macro dispersion calculated by stochastic analysis of independently measured heterogeneity, a well-known large-scale experiment was performed (known as MADE), which provided the investigation of large-scale hydraulic conductivity trends, sorption and process on solute transport (Boggs et al., 1992). To evaluate the performance of numerical contaminant transport models, the same experimental results were used (Zheng et al., 2011). Since 2000's, the use of tracers as investigative tool in hydrogeology has been increased, and they are used for the investigation of the advance transport phenomenon like colloid-facilitated transport, multispecies reactive transport and pore scale mixing. To quantify the subsurface volume and the interfacial area of nonaqueous phase liquid (NAPL), the phase-partitioning tracers have been used (Divine & McDonnell, 2005).

2.2 Types of tracers

The main two types of traces by their origin are artificial tracers and environmental tracers. The spatial and the temporal timescales of information provided by them is different (Cook, 2015)

2.2.1 Artificial tracers

The substances which are intentionally injected into the subsurface for the investigation purposes are known as artificial tracers. Artificial tracers are usually injected over a small area and the period between the injection and the observation is often measured in days. They are broadly used for calculating hyporheic exchange processes and provide useful information on rapid process such as identification of the flow path in karst aquifers. Conservative and non-conservative tracers are used to get information about the survival of viruses by using bacteriophage and to evaluate potential for sorption and degradation of the contaminants in the aquifer system. For estimation of hydraulic conductivity, flow velocity and dispersivity, heat and dyes are used as artificial tracers (Cook, 2015). Besides heat, dissolved ions, biological particles and dissolved gases are use used conventionally (Brennwald et al., 2022). Noble gases are found to be ideal tracers due to their properties of colourlessness, non-adsorption to the aquifers and not effecting the quality of groundwater negatively. Gas-equilibrium membrane-inlet mass spectrometers (GE-MIMS), a recently developed technology, provide effective on-site analysis of dissolved gases at high temporal resolution, although the cost remains prohibitive for routine studies.

2.2.2 Environmental tracers

Environmental tracers are naturally present in the groundwater or introduced by human activities. The information provided by them are usually on the process which occurred years ago. The tritium produced by the nuclear bomb explosion in the 1950's was found to be useful tool for investigation of thee groundwater. From 1960's to 1980's, the isotopic methods were the backbone of environmental tracer research. In the past few decades, the increase in the environmental tracers have been noticed, most of them are gases which are used for industrial purposes (chlorofluorocarbon).

The information provided by the environmental tracers are at larger spatial scales and they have been distributed over the earth surface. They are used for the detection of the leakages from large water systems, for measuring evaporation and the recharge rates of aquifers. They are used for identification of non-point contaminant sources in aquifers and provide information on chemical reactions for example denitrification and sulphate reduction. To estimate the residence time of groundwater is one of the important applications of these tracers, which helps in calculating the velocity of the water and the rate of recharge for the aquifers (Cook, 2015).

The limitation of the use of environmental tracers are that they require knowledge about the due to their spatial and temporal variability, which it is difficult to be estimated unless a large number of samples are collected. Moreover, the environmental conditions of subsurface (salinity, temperature, pH and Eh) may affect different tracers in different ways, so it is difficult to find a best tracer that could be used in any condition and environment. The interpretation of tracer tests and their accuracy may become complex due to their nonconservative behaviour (like sorption or degradation), thus compromising quantitative information regarding residence times.

2.3 Tracer test methods

The tracer test can be performed on laboratory scale and field scale. In the first one the tests are performed at local scale to estimate the subsurface parameters on point scales. This approach can be performed also at small scale field investigations e.g., the combination of dipole flowmeter with tracer injection. These methods are useful to understand the transport processes and for transport mode predictions. The effort required to collect an adequate information on local tracer movement is likely to be too high for ordinary field-scale modelling applications (Ptak et al., 2004).

The second strategy is to take the measurement of the subsurface parameters directly at field scale. This method may be used, in particular, in many hydrogeological situations where the costs of obtaining the input data required for stochastic simulations, the effort required to analyse the geostatistical data, and the computation time become prohibitively expensive or if some input parameters (for example, concentrations within the contaminant source zone) cannot be described using geostatistical methods. The obtained results can be used for predicting the transport, for reducing the uncertainty in the prediction of the stochastic modelling frameworks and for application of transport modelling methods (Ptak et al., 2004).

The tracers test can be performed in undisturbed groundwater flow field using the natural hydraulic gradient conditions or by ground water pumping or tracer solution injection in forced gradient conditions. Usually, the tracers are injected to the monitoring well and the related breakthrough curves are calculated.

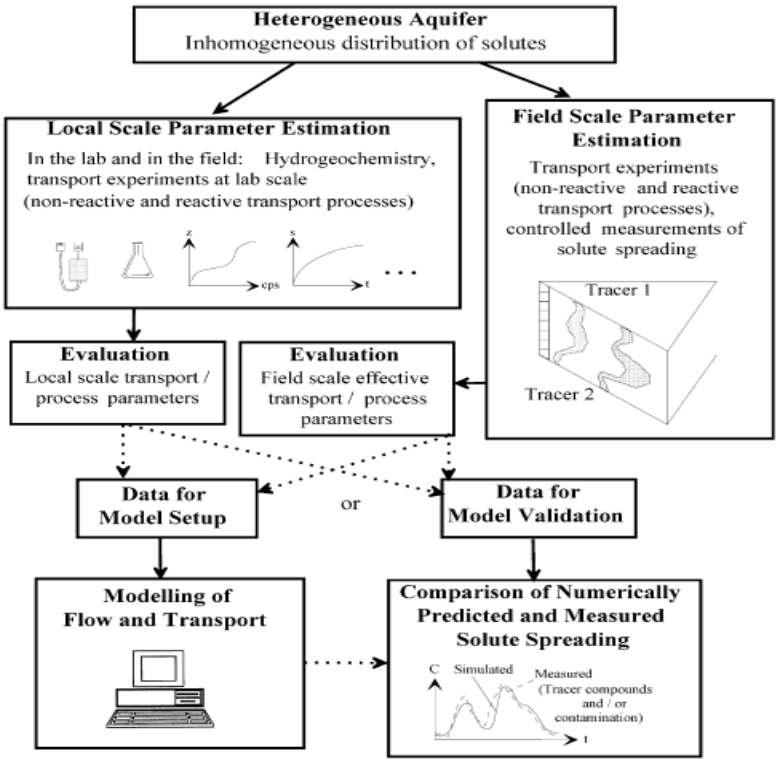

Figure 2. 1: Approaches for using tracer test-based data (Ptak et al., 2004)

The compounds used for tracer tests can be reactive or non-reactive, like ideal tracers which are used to investigate the transport of solutes due to their resistance to degradation. Keeping in mind the site-specific conditions, the ideal tracers can salt based like sodium chloride (NaCl), sodium bromide (NaBr) or fluorescent tracers such as Fluoresceine, Pyranine, radioactive tracers like Rn^{222} or Tritium and dissolved gases like He or H_2. Laboratory testing must be

performed to select the ideal or close to ideal trace behaviour compound in different aquifers matrices and redox environments (Ptak et al., 2004).

2.3.1 Natural gradient tracers (NGTT)

In the natural gradient tracer test (NGTT), for a limited period the tracer solution is injected at field scale to the undisturbed groundwater flow field. In the downstream direction, the measurement of depth integrated breakthrough curves is achieved in the monitoring wells. Knowledge about the direction of estimated mean transport and average transport velocity is required, for performing productive experiment and for planning of sampling activities. The main advantage of the test is the detection scale is not limited by principle and the groundwater flow is due to natural gradient without any requirement of pumping (Garabedian et al., 1991).

The limitations of the NGTT are, if the distance to be investigated is very large and the groundwater flow velocity is small, the test may become extremely long (years) and thus much more experimental monitoring efforts are required. Also, there are difficulties in measuring the breakthrough curves because of the shift in groundwater flow direction due to changes in the boundary conditions (Chen et al., 2012). Moreover, an elevated spatial resolution of monitoring wells is required for the characterization of the solute plume in the heterogenous aquifers. The duration of the experiment become relatively longer, when some types of reactive tracers are injected (Ptak et al., 2004).

2.3.2 Force gradient tracer test (FGTT)

FGTT provides well-defined experimental conditions due to the force gradient and the experimental duration is reduced. These tests can be performed in different situations of groundwater flow fields such as convergent (Push-pull tests), divergent, and in a dipole type groundwater flow field. Groundwater is continuously pumped into an injection well in the divergent flow field approach and the addition of tracers is done continuously for a limited time with mixing in the well, after reaching the quasi-steady-state flow. The depth integrated or multilevel tracer breakthrough curves are measured in the surrounding monitoring wells in all direction using a single tracer (Ptak et al., 2004).

In the convergent flow field technique, the tracer is continually injected as groundwater is pumped out of an extraction well for limited time and the breakthrough curves are achieved at

the extraction point (Colombani et al., 2015). In pumping well, it is also possible to measure the multilevel breakthrough curves by using flow separation technique (Ptak et al., 2004).

In the dipole flow field approach, the extracted groundwater from one well is reinserted in another well. After which, the tracer is injected to the infiltration well within dipole (pulse with recirculation) and monitored at a specific site which can be the extraction well or sampling location between the wells. The groundwater extraction and infiltration rates are found to similar in the symmetrical set-up. Long experimental time may be required to obtain satisfying tracer recovery based on the nature of dipole flow field and it can be improved by increasing the extraction rate. The advantage of the divergent and convergent flow field is the possibility of recovery of tracer (Ptak et al., 2004). The advantages of FGGT includes, the short period of the experiment reducing the effect of hydraulic gradient variations, possibility of using several transport directions by using on single trace, possibility to calculate the mass balance and the use of reactive tracers at affordable expenses. The disadvantages include the limitation of the scale of detection, treatment of the pumped ground water and energy requirement for pumping due to absence of natural ground slope (Ptak et al., 2004).

2.3.3 Multi-tracer approach and DNA sequence-based tracers

To reduce the cost and the efforts of the experiments, multiple tracer tracers can be used in a single experiment which also gives more information (Moeck et a., 2017). However, the maximum number of tracers that can be used parallel with each other can be 8 to 10, because of the physical and hydrogeochemical properties of the commonly used tracers such as salt or gas tracers and due to limitations of sampling and analysis procedures. For this, several analytical techniques such as fluorescence spectrometer, wet chemistry, ion chromatography and mass spectrometry can be used (Ptak et al., 2004).

DNA molecules with individually coded information were developed in the end of 20th century, by which it become possible to carry out multi-tracer experiments with unlimited number of locations. It consists of subunits known as nucleotide which is made of nitrogenous bases and a sugar skeleton. The nucleotide sequences (shorter or longer) can be designed by chemical synthesis. The length of the synthetic DNA molecules, which in the instance of the field case study provided is 90 nucleotides, is significantly shorter than that of natural single-stranded DNA molecules.

The sorption of DNA molecules depends on the type of aquifer material as well as the physical and chemical characteristics of the groundwater since the DNA molecule is an anion, with a negative charge synthetically suited to the requirements (Aquilanti et al., 2015). It has been demonstrated that clay minerals have a far better capacity for adsorption than sand grains. Salt concentration, pH, and cationic valence all have a direct impact on adsorption of DNA molecules (Pang et al., 2020). The bacterial activities enhanced the degradation of the DNA molecules, thus their suitability as tracers may be questioned and still more research is required for the dependency of DNA molecules on the site specific physical and hydrogeochemical conditions (Ptak et al., 2004).

DNA tracking has the potential to be an effective tool for (three-dimensional) subsurface research at various sizes of investigation. To build evaluation methodologies and modelling tools for the interpretation of the measurements, as well as to acquire a thorough knowledge and quantification of the (reactive) tracer-aquifer material interaction processes; although more thorough laboratory and field experiments are required (Ptak et al., 2004).

3 Material and Methods

The study was performed sequentially on (i) batch experiments in no flow conditions to quantify the mass loading rate of saline solution through the polylactic acid (PLA) bag, (ii) in column experiments of 5 cm internal diameter to mimic the one-dimensional flow within a monitoring well and (iii) a large tank in controlled laboratory conditions in SIMAU department of "Università Politecnica delle Marche".

3.1 Laboratory Instruments

3.1.1 Design of Tank

At Università Politecnica delle Marche's Hydrogeological Laboratory (SIMAU), a large tank was set up for the simulation of the natural conditions. The tank, having the dimensions of 1.4 m x 4.0 m x 1.3 m, was constructed with armed PVC on inner side and secured with external structure made of natural wood with steel scaffolding pipes. It was filled with the coarse sand materials, in which 9 m^3 was sandy sediments while 0.5 m^3 of gravels. The sandy sediments for the experiments were collected from a sand pit located in the alluvial plain near the Esino river in Ancona, Italy, the materials were transferred in the laboratory via a mini scraper and the tank was filled from the inflow side toward the outflow, till it reaches the height of 1.1±0.02 m. The materials were compacted artificially by using a shovel and then naturally with continuous monitoring for two months under saturated conditions. The compaction was found to be negligible once an initial localized collapse was identified near the infiltration point. The probes were placed at the monitoring wells **A2, B2, C2** and **D2**, and at the outlet of the tank (**Out**), the horizontal distances between them are listed in **table 3.1**.

Table 3. 1: Horizontal distance of probes from each other.

Probes	Distance (m)
A2-B2	0.5
A2-C2	1.5
A2-D2	3
A2-Out	3.5
B2-C2	1
B2-D2	2.5
B2-Out	3
C2-D2	1.5
C2-Out	2
D2-Out	0.5

3.1.2 Wells and piezometers

Twelve piezometers were installed in the tank in a way to form a semi-regular grid, out of which eight piezometers were having the bottom with screen length of 5 cm length while the remaining four were completely screened wells as shown in fig 3.1.

Figure 3. 1: 3D tank in hydrogeological laboratory, SIMAU,

The internal diameter of the monitoring wells in the center of tank was 5 cm. The monitoring wells were equipped with high resolution multi-level samplers (MLSs), and they consist of 6

HDPE tubes having internal diameter of 4 mm placed around the wells as shown in the Figure 3.2. The tubes were connected to a micro-screen having length of 5 cm and the samples ports were evenly distributed every 10 cm, beginning at the bottom of the tank and extending up to 60 cm.

Figure 3. 2: HDPE tubes around the monitoring wells

3.1.3 Data loggers and monitoring probes

Freatimeter (Pasi, Città di Castello, Italy) was used to obtain the groundwater measurements, which was done by inserting the probe inside piezometers. The warning system is activated by the contact of the sensors with the water surface leading to formation of a close circuit is formed, allowing the operator to note the depth of groundwater by using a graduated cable. To minimize the perturbation of the experiment, the salinity is measured only one using the MLSs, thought groundwater heads, electrical conductivity and the temperature is measured using Soil & Water Diver® water level data logger (Eijkelkamp, Giesbeek, The Netherlands) with an interval of 10 minutes. The latter is the most used instrument for measuring groundwater level, electrical conductivity, and temperature. The noticeable features of this equipment are, its availability in different sizes, having no mechanical parts, resistant to wear and tear, reading can be taken on site with DC cable, no air vent, data can be transfer easily in the software using different output formats, barometric logs of air pressure variation, can be used both for wells or in the open water (Eijkelkamp Foundation, 2011). Corrections must made for the changes

in the atmospheric pressure using the Barologger® (Eijkelkamp, Giesbeek, The Netherlands), which is positioned at the soil surface.

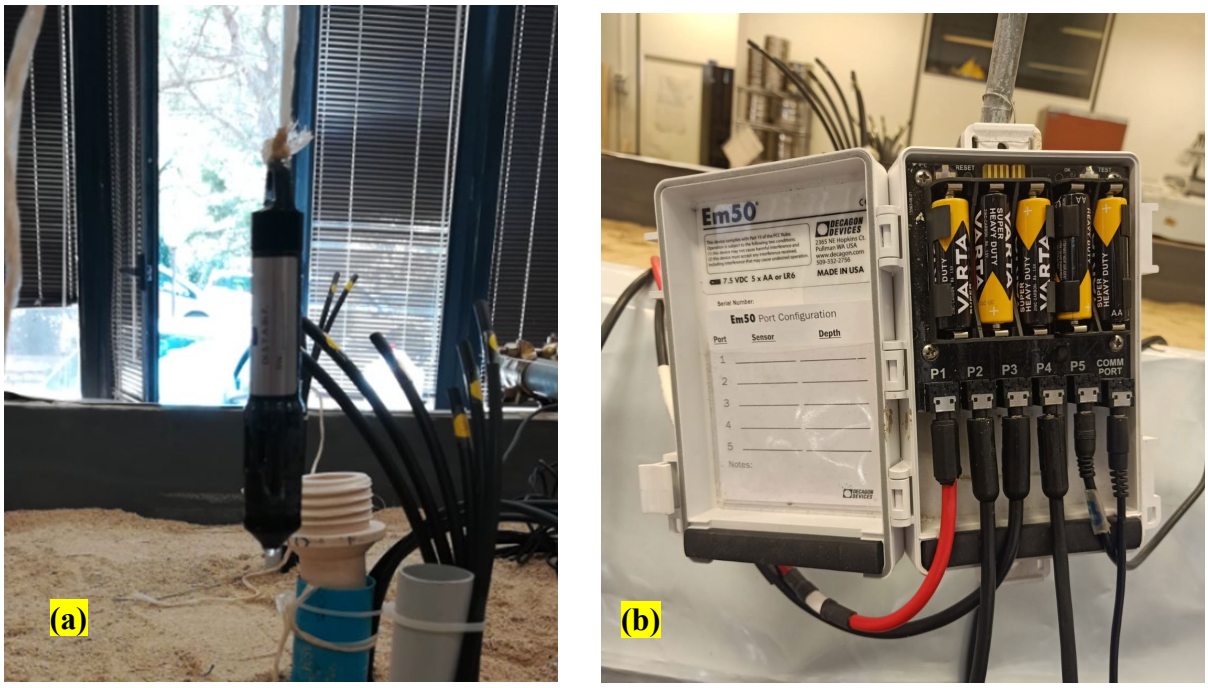

Figure 3. 3: (a) Soil & Water Diver water level data-logger, (b) Em 50 data logger (Decagon devices)

A 5TE® Meter probe (Meter Environment, Pullman, WA, USA) was used in vadose zone for monitoring the volumetric water content (VWC), temperature, soil bulk electrical conductivity. The probes have been installed in the tank respectively at 5 and was connected to the meter data logger (ECH2O) having interval of recording as 10 minutes.

Figure 3. 4: 5TE probe Decagon.

To monitor the bulk electrical conductivity, temperature of soil and volumetric water content Decagon 5TE soil moisture sensor. In the water limited areas, the importance of the monitoring salt level is the same as monitoring soil moisture. The salt levels are measured with the help of bulk electrical conductivity. The table represents the following data (Pessl instruments, 1984).

Table 3. 2: meter group ECH20 5TE soil moisture sensor features

Volumetric water content (VWC)	**Range**	Mineral soil calibration: 0.0-0.1 m3/m3
		Soilless media calibration: 0.0-1.0 m3/m3
		Apparent dielectric permittivity: 1 (air) to 80 (water)
	Resolution	0.0008 m3/m3 from 0%-50% VWC
	Accuracy	Generic calibration: ± 0.03 m3/m3
		Medium-specific calibration: ± 0.02 m3/m3
		Apparent dielectric permittivity: 1-40 (soil range), ±1 εa (unitless) 40–80, 15% measurement
Temperature	**Range**	–40 to +60 °C
	Resolution	0.1 °C
	Accuracy	±1 °C
Bulk electrical conductivity (EC)	**Range**	0–23 dS/m (bulk)
	Resolution	0.01 dS/m from 0–7 dS/m, 0.05 dS/m from 7–23 dS/m
	Accuracy	±10% from 0–7 dS/m, user calibration required from 7–23 dS/m
Dimensions		10.9 cm (4.3 in) lenght; 3.4 cm (1.3 in) width; 1.0 cm (0.4 in) height
Prong length		5.0 cm (1.9 in)
Operating temperature range		-40 °C to 60 °C
Cable length		5 m (standard)
Supply voltage		3.6 VDC to 15.0 VDC
Current drain (asleep)		Typical: 0.03 mA
Current drain (measurement)		0.5 mA to 10.0 mA (typical: 3.0 mA)
Measurement duration		Typical: 150 ms; Maximum: 200 ms

3.1.4 Physical parameters and hydraulic properties

Dry sieving and gravimetric measurement of 5 samples were done, by which the physical parameters like grain size, bulk density and porosity were determined. A randomly selected soil sample from the tank was oven dried for 105 °C for 24 hours and sieving analysis was performed. The sieves were placed on the mechanical shaker having the larger mesh size on the top and the smallest mesh size at the bottom as shown in figure 3.3. The retaining material on each sieve is weighed, after the shaking is completed. To calculate the percentage of retained on each sieve, divide the mass retained on each sieve by the total mass of the sample. The particle size is determined by the mass retained on specific sieve in the percentage. From table 3.2, it can be noticed that there is a small variability in the grain size distribution with low coefficient of uniformity. According to Wentworth classification, the sample was identified as coarse-medium sands. Furthermore, using rate pumping test, slug tests and Kozeny-Carman formula (Freeze & Cherry, 1979; Rosas et al., 2014), the hydraulic conductivity was determined previous studies on the same three-dimensional tank.

To compare hydraulic conductivity (K) of an unconsolidated geologic material with the grain size distribution achieved from the sieve analysis, different empirical formulas are proposed. For estimation of K, two metrics from the grain size distribution plots were uses (D_{10} and D_{60}). D_{10} is referred to as effective dimeter while the ratio of D_{60} to D_{10} is known as coefficient of uniformity.

To estimate the hydraulic conductivity of sediments and soils, The equation of Kozeny and Carmen that has been used:

$$K_{KC} = C_{KC}\frac{g}{\nu}\frac{n^3}{(1-n)^2}D_{10}^2$$

where

$-$ K_{KC} is hydraulic conductivity (m/s).

- C_{KC} is an empirical coefficient equal to 1/180 [dimensionless].

- g is gravitational acceleration (m/s²).

- ν is kinematic viscosity of water (m²/s).

- n is total porosity (-).

This formula is assumed to be valid for sediments and soils composed of silt, sand and gravelly sand.

Finally, from Marche Region Meteorological Hydrogeological Information System (SIRMIP, 2020) website, the data regarding relative humidity was collected for every 30 minutes.

Figure 3. 4: Column of sieves placed in a mechanical shaker.

Table 3. 3: Parameters of sediments and their standard deviation.

Parameter	Tank sediments
Sand (0.63-2 mm)	98.5±8.6
Silt (2-63 µm)	1.4±1.7
Clay (<2 µm)	0.1±0.1
Dry bulk density (kg/dm3)	1.68±0.1
Residual water content (%)	0.05±0.01
Saturated water content (%)	29.1±1.7
CU (-)	3.1±1.6
D10 (mm)	0.45±0.24
D60 (mm)	1.09±0.17

3.1.5 Biodegradable plastic bags (PLA)

Biodegradable plastics were used as a cost-effective exchange membrane. A sample of sodium chloride salt (NaCl) was inserted in the biodegradable plastic bags, after which it was introduced to the monitoring well A2.

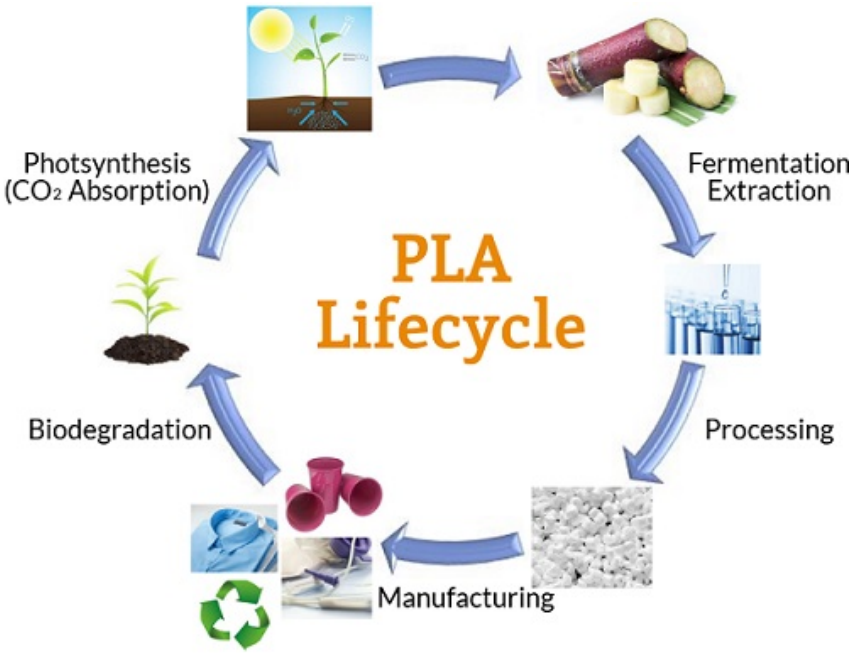

Figure 3. 5: Life cycle of PLA.

The bags are Polylactide (PLA), thermoplastic polyester which is obtained by the condensation of lactic acid with the loss of water. Another way to obtain is by ring-opening polymerization of lactide. The chemical formula is $(C_3H_4O_2)_n$. Fermented plant such as corn, cassava, sugarcane and sugar beet pulp are used as the main sources for its production. Its popularity is due to its economic production from renewable resources and its consumption as a bioplastic reached second highest in the world by 2010.

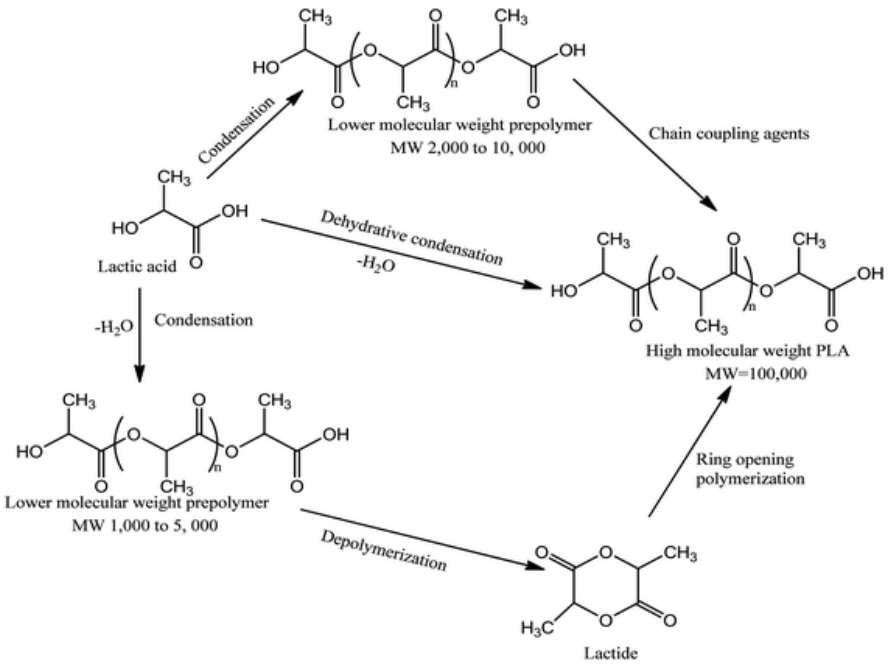

Figure 3. 6: Methods for PLA production.

PLA can also be used for 3D printing due to its properties like low melting point, high strength, low thermal expansion, and high resistance to heat. It is also used for making disposable cutlery and kitchen appliances. Moreover, it is used compost bags, food packaging and loose-fill packaging material.

Table 3. 4: Physical and mechanical properties of PLA.

Property	Value
Melting temperature	130-180 °C (can be increased 40-50 °C)
Young Modulus	2.7-16 GPa
Heat resistant	110 °C (Increasable by 60 °C)
Heat deflection temperature (HDT)	52 °C
Density	1.24 g/cm^3
Tensile strength	50 MPa
Flexural strength	80 MPa
Impact strength (Unnotched) (J/m)	96.1
Shrink rate	0.37-0.41 %

Figure 3. 7: PLA biodegradable plastic bag as an exchange membrane for NaCl Salt.

3.1.6 Other Instruments used

To measure the temperature, electrical conductivity in the outlet of thank and for the one-dimensional column experiment, Diver data logger was used, and the data was exported using the Diver office 2014.1 software.

For pumping the water to the graduated cylinder in the one-dimensional column experiment, peristatic pump (MINIPULS® 3 Gilson) was used.

Figure 3. 8: (a) Data logger used in outlet of the tank, (b) Peristatic pump (MINIPULS® 3 Gilson)

To measure the pressure in the surrounding of the tank, BARO-diver is placed on the surface of the sand in the tank. It continuously records the variations in the atmospheric pressure.

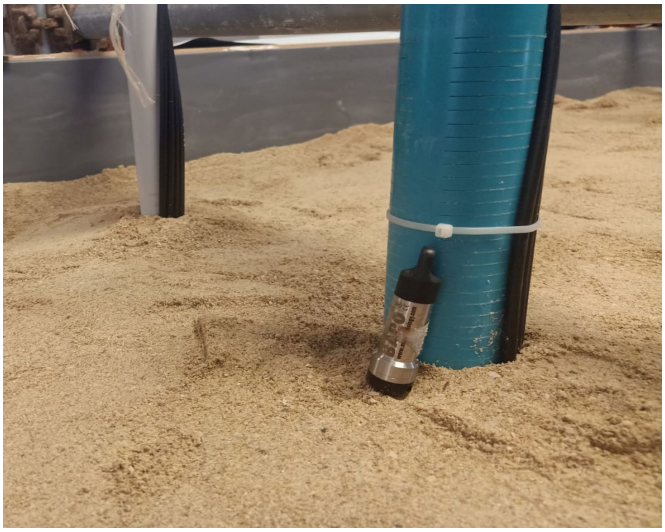

Figure 3. 9: BARO-Diver for recording the atmospheric pressure

3.2 Experiments

Different experiments were formed based on the flow dimension (batch, 1D, 3D), the flow conditions and velocity, introduction of biodegradable PLA plastic as an exchange membrane and single well experiment. They are briefly explained which are explained below.

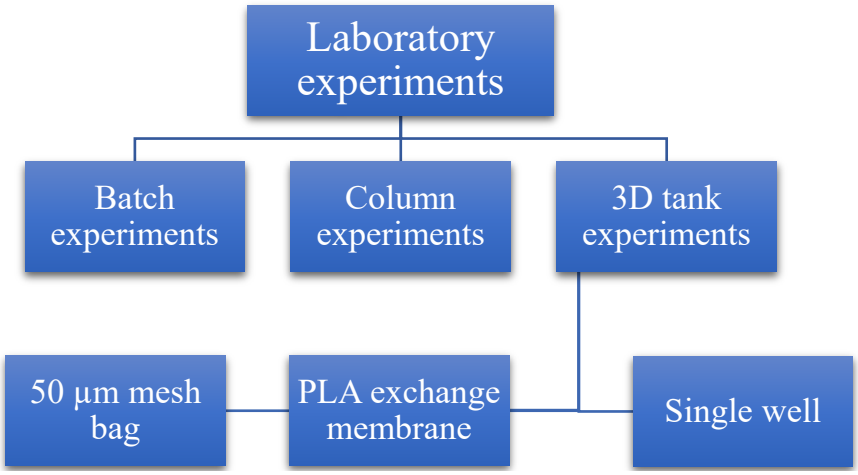

Figure 3. 10: Flow diagram of the laboratory experiments performed.

3.2.1 Batch experiments (No flow conditions)

The experiment was performed to quantify the exchange rate of the salt among the membrane which is made of PLA. The 50 g of NaCl salt was inserted and put in a PLA bag. The salt was weighted and then inserted to a one-dimensional water column. The data logger was calibrated and inserted in the water column to check the electrical conductivity. The experiment was performed two times to verify the accuracy of the exchange membranes.

3.2.2 Column experiment (With different flows)

The experiment was performed to check the efficiency of the membrane with flow in one dimensional column. Known amount of sodium chloride salt was filled into the membrane (plastic bag). A graduated cylinder was filled with 100 ml of water. The membrane along with the data logger already calibrated were introduced to the graduated cylinder and the water was continuously entering to the cylinder using peristatic pump (MINIPULS® 3 Gilson) and overflowing from the cylinder. The experiments were performed at different flowrates (slow and fast).

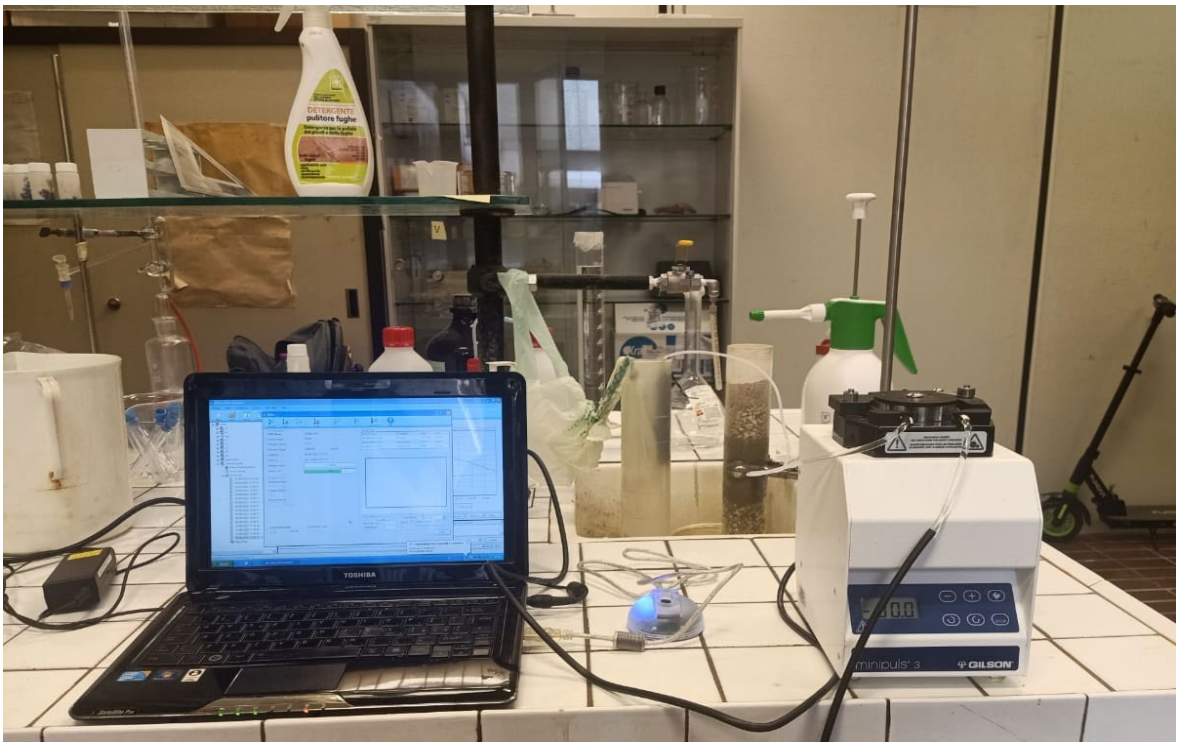

Figure 3. 11: 1-D experimental setup and apparatus

3.2.3 Tank Experiments

Three experiments were performed using the 3-dimensional tank in the controlled laboratory conditions. In the first experiment the NaCl salt crystal was directly inserted to the monitoring well, electrical conductivity and temperature were the main tracers. The probes were inserted in the monitoring wells to record the temperature, water level and electrical conductivity at regular interval time of 10 minutes. A probe was inserted directly in the soil to check the moisture content of the soil. Water was entering to the reservoir by a constant head reservoir

continuously and was flushing out through the outlet. The data was recorded continuously and was transferred to the excel file using ECH2O software.

In the second experiment same tank was used but the NaCl salt was introduced using the exchange membrane. The salt was inserted in the monitoring well A2, data were recorded until reaching breakthrough curves and for the flow to become steady. The horizontal flow velocity was calculated from the time required to reach the breakthrough curves of different monitoring points.

Finally in the third experiment, all the probes were transferred to a single monitoring to check the vertical direction of flow. The salt source was introduced to the monitoring well using the PLA plastic bag. The data was recorded continuously till breakthrough curves and the steady state were achieved. Moreover, the salt source was then removed, and the data were continuously recorded to check the recovery of the salt mass.

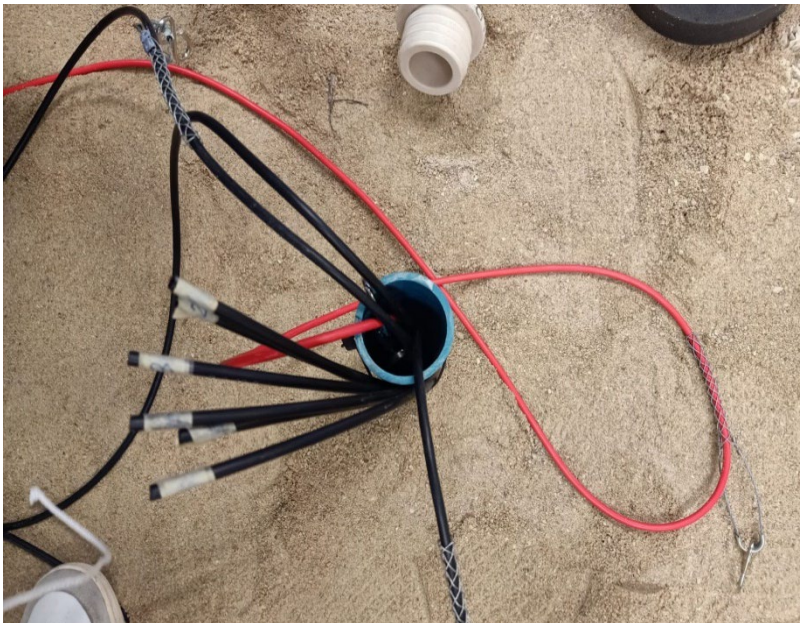

Figure 3. 12: Single monitoring well test for checking the vertical flow velocity.

4 Results and discussion

4.1 Batch experiment (no flow conditions)

The experiment was performed to quantify the exchange rate of the NaCl salt among the membrane which is made of PLA. The NaCl salt was weighted (50 g) and put in a PLA bag. The PLA bag including the salt was then inserted to a one-dimensional water column. A portable conductimetry was calibrated and inserted in the water column to record the variation in electrical conductivity (EC) with the time interval of 10 minutes at initial stages and at later stages was then recorded less frequently. The experiment was performed two times in order to verify the accuracy of the exchange membrane (PLA) and to check whether it replicates the same trend line of EC.

The time duration for the first experiment was 28 hours, while for the second experiment the duration was 25 hours. At the end of the experiments, the EC (EC) data were inserted in Excel software to plot the EC values versus time. The values of the variation of EC with respect to time are listed in table 4.1 and graphically presented in figure 4.1.

Table 4. 1: Time variation of EC through the diffusion from PLA bag.

Batch experiment 01		Batch experiment 02	
Time (min)	EC (µS/cm)	Time (min)	EC (µS/cm)
0	250	0	252
20	260	20	263
30	270	40	275
60	290	60	280
90	305	460	580
120	330	800	780
240	400	1000	908
480	580	1500	1350
800	810		
1200	1150		
1700	1550		

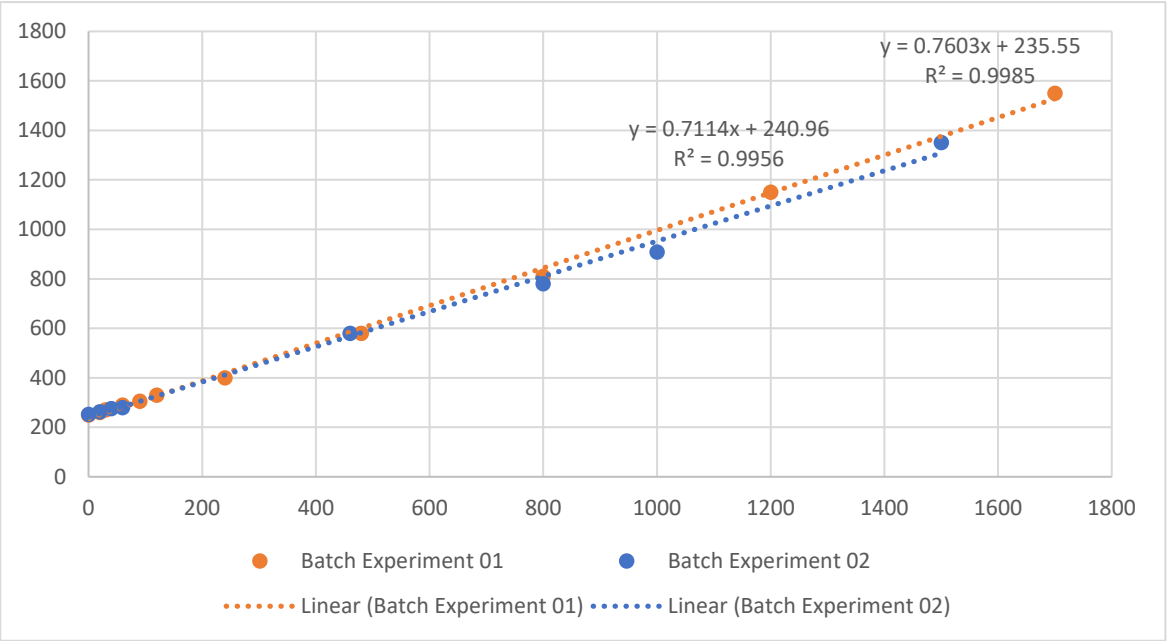

Figure 4. 1: Time variation of electrical conductivity.

By the figure 4.1 presented above, a linear trend of the variation of EC with respect to time can be noticed. Before start of the experiment, the EC recorded was 250 (µS/cm), and it kept increasing linearly with time and by the end of the experiment, it reached to a maximum value of 1550 (µS/cm).

The second experiment was performed to confirm the diffusion of salt from PLA bag and to verify the trend line is repeated in similar way or not. This time the duration of the experiment was 25 hours and the value of EC recorded at the start of the experiment was 252 (µS/cm) and at the end of experiment the recorded value of EC by the data logger was 1350 (µS/cm). The graph shows the same variation of the EC.

The zero-order exchange rate (linear) has been derived from the slope of the best fitting line which provided very high R^2 values in both experiments (greater than 0.99). The exchange rate is approximately 0.74 µS/cm/min which is equivalent to 1060 µS/cm/d.

Based on the results of these two batch experiments, it can be noticed that the biodegradable plastic bag (PLA) allows the process of NaCl diffusion and further lab experiment can be continued using it as an exchange membrane in the tracer test to ensure a source of tracer with a well-known mass loading rate. Furthermore, the PLA bag was kept more than a month to check the degradation or damage to the bag, but it was found to be in good condition, and this make it suitable to be employed safely for at least a week as continuous source of tracer.

4.2 Column experiment

After confirmation of the exchange properties of the PLA bag, three lab experiments were performed to check the exchange rate of the PLA bag using the one-dimensional column with different flow rates. 50 grams of NaCl salt was inserted to PLA bag. Graduated cylinder was filled with 100 ml of water. A portable conductimetry was calibrated and inserted in the water column to record the variation in EC with the time interval of 1 second at initial stages and at later stages was then recorded with time interval of 5 minutes. To pump the flow to the graduated cylinder from a reservoir, peristatic pump was used.

To check the effect of flow on the variation of EC, three experiments were performed at different flowrates, maximum flowrate (18 mL/min), at 9 mL/min and at a low flow rate of 3 mL/min.

The experiment at the maximum flowrate was performed for the duration of 3844 seconds (64 minutes) with the interval of 1 seconds for recording the data. In the start of the experiment the EC was recorded 576 (µS/cm) and it reaches to the maximum value of 604 (µS/cm). The variation of EC with respect to time is plotted in figure 4.2.

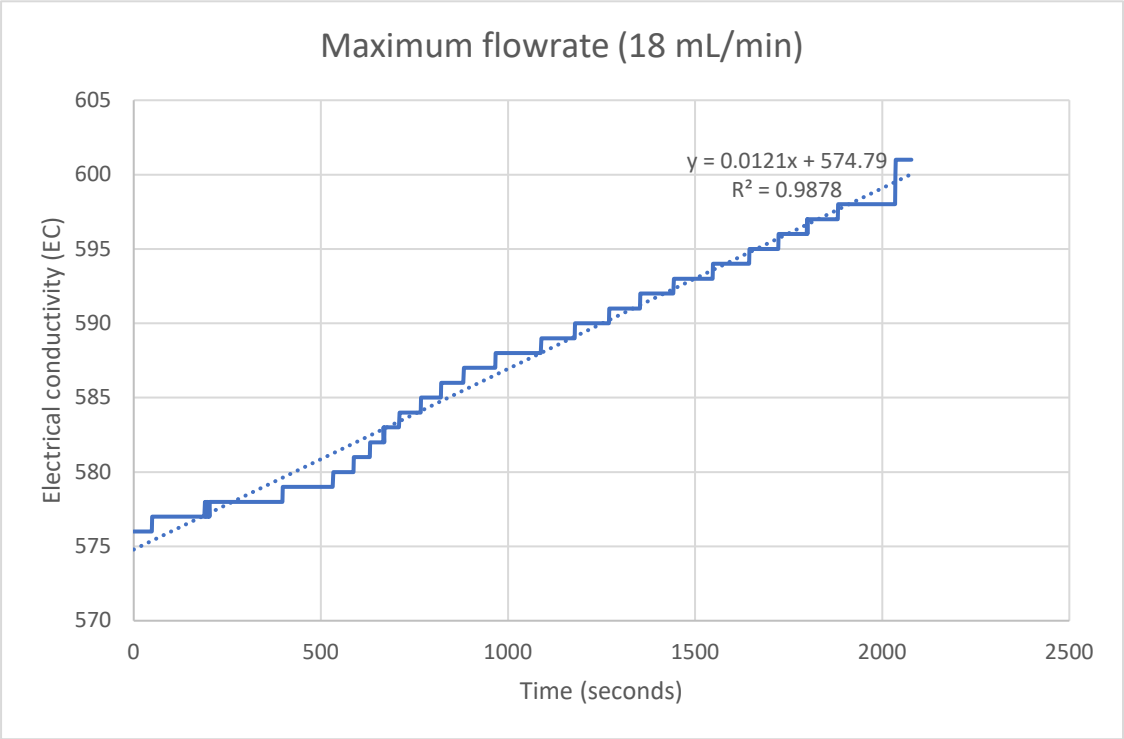

Figure 4. 2: Time variation of electrical conductivity with flowrate of 18 mL/min.

In the second experiment, the flowrate was halved, and the variation of EC was recorded at time interval of 300 seconds (5 minutes) and the total duration of the experiment was 54000 seconds (900 minutes or 15 hours). The EC of the water was 525 (µS/cm) at the start and it reached the maximum value of 607 (µS/cm). The results are presented graphically in figure 4.3.

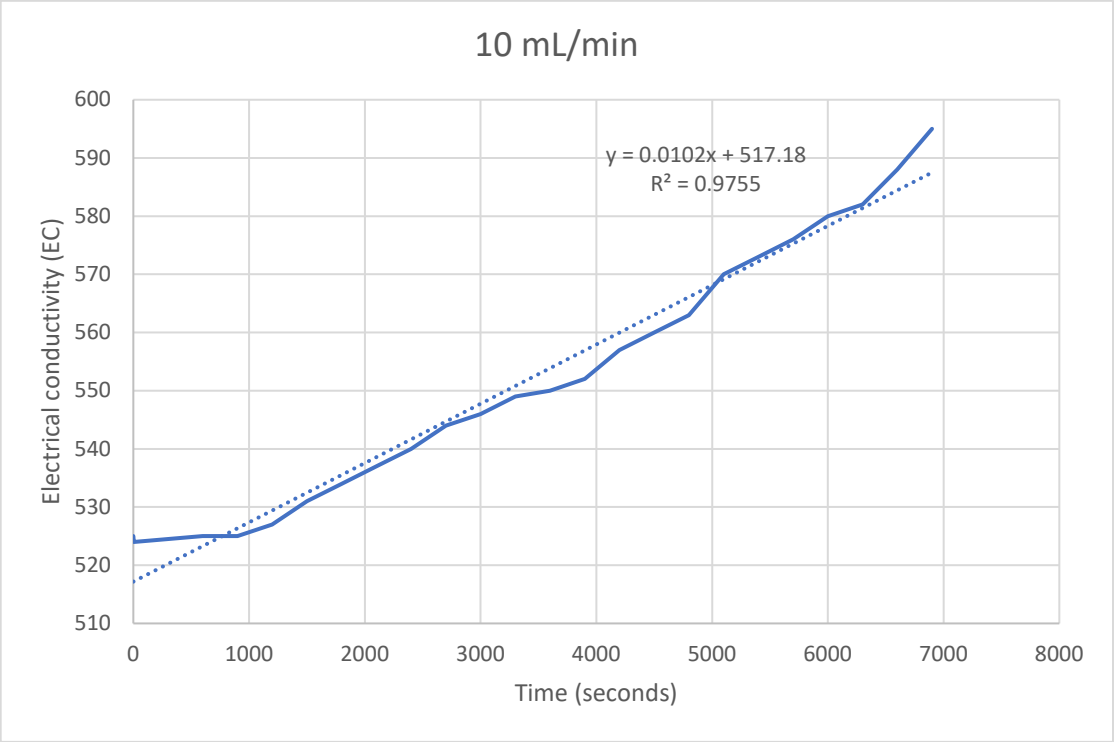

Figure 4. 3: Time variation of electrical conductivity with flowrate of 10 mL/min

The third experiment was performed at lower flowrate of 3 mL/min and the same time interval of 5 minutes was kept for recording the data. The total duration for the experiment was 96300 seconds (1605 minutes or 26.75 hours). The EC of the water was 629 (µS/cm) at the start of the experiment and it reached the maximum value of 717 (µS/cm). The results are presented graphically in figure 4.4.

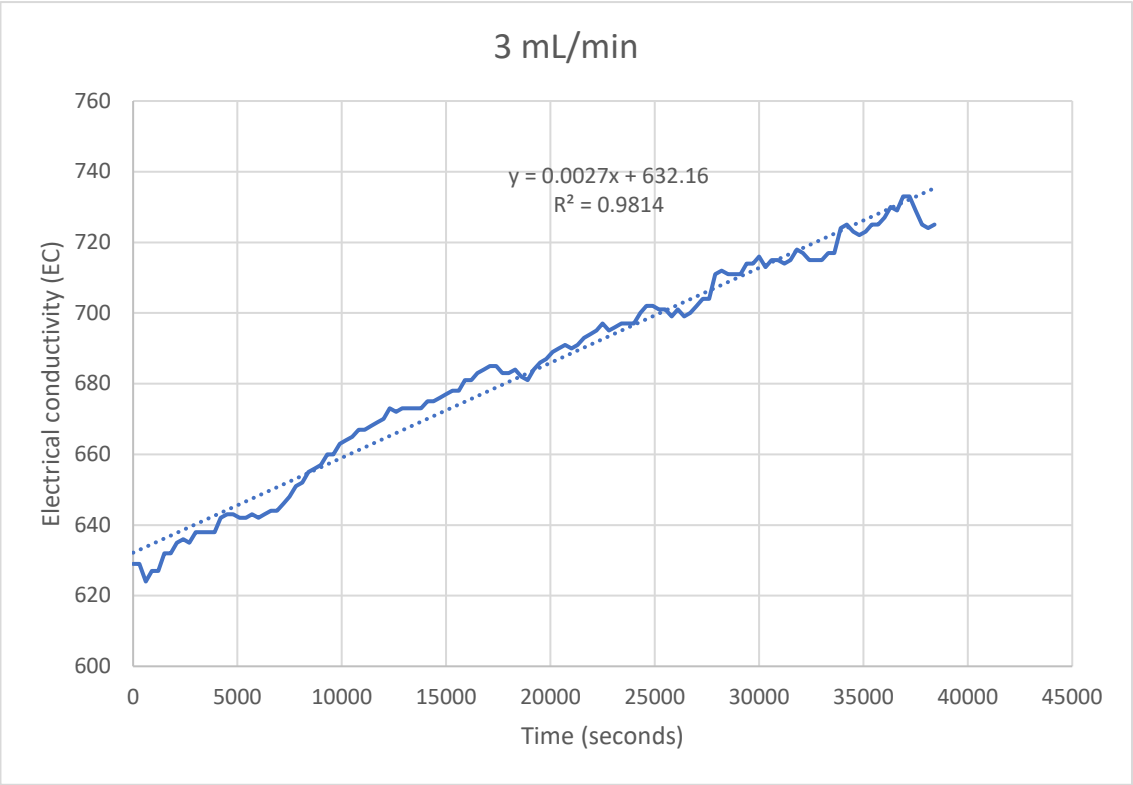

Figure 4. 4: Time variation of electrical conductivity with the flowrate of 3 mL/min.

The zero-order exchange rate, or NaCl mass loading rate (MLR) has been derived from the slope of the best fitting line which provided very high R^2 values in all experiments (0.988, 0.987 & 0.981). The MLR for the maximum flowrate was approximately 0.0121 µS/cm/s which is equivalent to 1045 µS/cm/d, while for intermediate flow rate was 0.0102 µS/cm/s which is equivalent to 881 µS/cm/d. For the final experiment with lowest flowrate, the MLR was approximately 0.0027 µS/cm/s which is equivalent to 233 µS/cm/d.

Furthermore, the velocities for different flowrates were calculated by know the area of the column (18 cm^2) used in the experiment. The specific discharge calculated was 1 cm/min (14.4 m/d), 0.56 cm/min (8.0 m/d) and 0.166 cm/min (2.4 m/d). The results are listed in table 4.2.

Table 4. 2: Calculation of specific discharge.

Calculation of Specific discharge				
S.NO	Flowrate (cm^3/min)	Area of the Column (cm^2)	Velocity (cm/min)	Velocity (m/d)
1	18	18	1.00	14.4
2	10	18	0.56	8
3	3	18	0.17	2.4

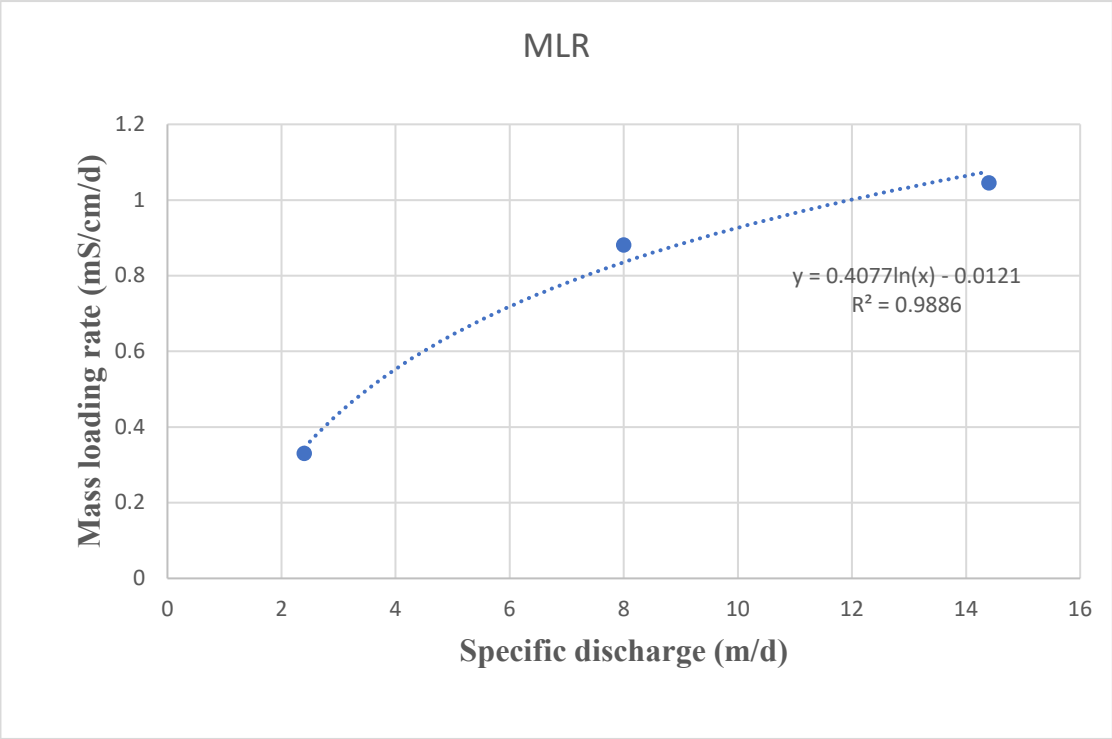

Figure 4. 5: Mass loading rate versus specific discharge.

Figure 4.5 shows the effect of specific discharge on the mass loading rate (MLR). The best fitting curve (logarithmic) was obtained with high value of $R^2 = 0.98$. Following logarithmic growth, a very rapid increase (linear) is noticed in the MLR at the start when specific discharge increases from 240 cm/d to 800 cm/d, after which MLR increases slightly by increasing the specific discharge.

Moreover, by the comparison of EC variation of different flowrate, it was noticed that the rate of increase of EC is higher at maximum flowrate than the slower flowrate, and it can be concluded that the NaCl MLR was triggered by advective transport rather than diffusion.

Conclusively, keeping an eye on the results obtained in the figure 4.4, PLA bag can be considered a good candidate to be used as an exchange membrane due to its low MLR efficiency for the NaCl release, because in the tracer testing techniques the priority is to choose a membrane which can release the solute at a low rate without changing the density and viscosity of water.

4.3 Tank experiment

4.3.1 Tank experiment without osmotic exchange bags

The study was performed on a large tank (1.4 m x 4.0 m x 1.3 m) in controlled laboratory conditions. The probes were placed at the monitoring wells **A2, B2, C2** and **D2**, and at the outlet of the tank (**Out**). A NaCl salt crystal of 170 g was inserted within the monitoring well A2, with the aim to reproduce a constant source of tracer via slow dissolution of the salt, by which EC (EC) increased rapidly as can be noticed in figure 2. EC and temperature were the main tracers in the performed experiment. The average velocity was found by the change in the temperature and EC at the points with respect to the time.

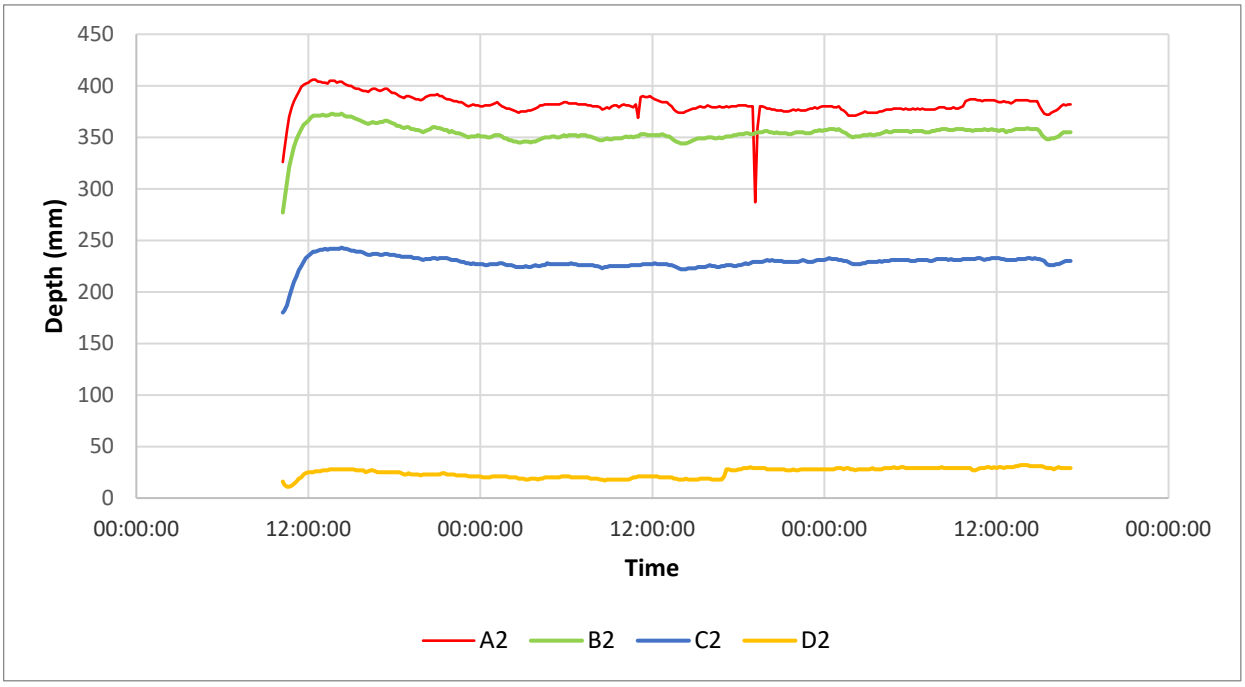

Figure 4. 6: Water level for the points A2, B2, C2 and D2.

The source was injected at A2 and was monitored continuously for 3.5 days for temperature, EC, and water level.

In tracer test it important to keep the flow and hydraulic gradient steady to provide constant boundary conditions to simplify the overall analysis. In figure 4.6, it can be noticed that the water level in the tank increased in the beginning of the experiment due to filling of the tank. At the point of NaCl injection there was slight perturbation of the water level due to the slow insertion of the NaCl crystal within the monitoring well A2, then a sudden decrease in the water level is visible due to the reason that the injection source was rapidly removed and then reallocated within the well A2.

The water level at A2 was on average 382 mm while in B2 was on average 354 mm, in C2 was on average 229 mm, in D2 was on average 26 mm. There are some instrumental fluctuations, but they are acceptable as per accuracy of the instrument (see the Materials and Methods section).

The average head gradient between the monitoring wells have been calculated and the values are listed in the table 4.3.

Table 4. 3: Hydraulic gradient between the monitoring wells.

Hydraulic gradient				
Monitoring Wells	horizontal distance	Δh		Hydraulic gradient (m/m)
		mm	m	
A2-B2	0.5	28	0.03	0.056
A2-C2	1.5	153	0.15	0.102
A2-D2	3	356	0.36	0.119
B2-C2	1	125	0.13	0.125
B2-D2	2.5	329	0.33	0.131
C2-D2	0.5	204	0.20	0.407

The effective velocities between monitoring wells were calculated using the Darcy Law in the form of:

$$v = \frac{K \times \vec{\imath}}{n_e}$$

Where K is the hydraulic conductivity (m/d), $\vec{\imath}$ is the head gradient and n_e is the effective porosity.

In particular, the average K value retrieved from the slug tests in each monitoring well is 34.5 m/d (Colombani et al., 2021), while the average n_e value is 0.2 (Alessandrino et al., 2022).

Table 4. 4: Velocities calculated from Darcy Law.

Monitoring wells	Hydraulic conductivity (m/d)	Porosity (m^3/m^3)	Head Gradient (m/m)	Darcy velocity (m/d)	Effective velocity (m/d)
A2-B2	34.5	0.2	0.056	1.92	9.58
A2-C2	34.5	0.2	0.102	3.51	17.57
A2-D2	34.5	0.2	0.119	4.10	20.49
B2-C2	34.5	0.2	0.125	4.31	21.56
B2-D2	34.5	0.2	0.131	4.53	22.67
C2-D2	34.5	0.2	0.136	4.68	23.41

It can be noticed that the average effective velocity is about 19.2 m/d which means that the average retention time in the tank should be 0.208 days or 5 hours, moreover the effective velocity increases towards the outflow of the tank.

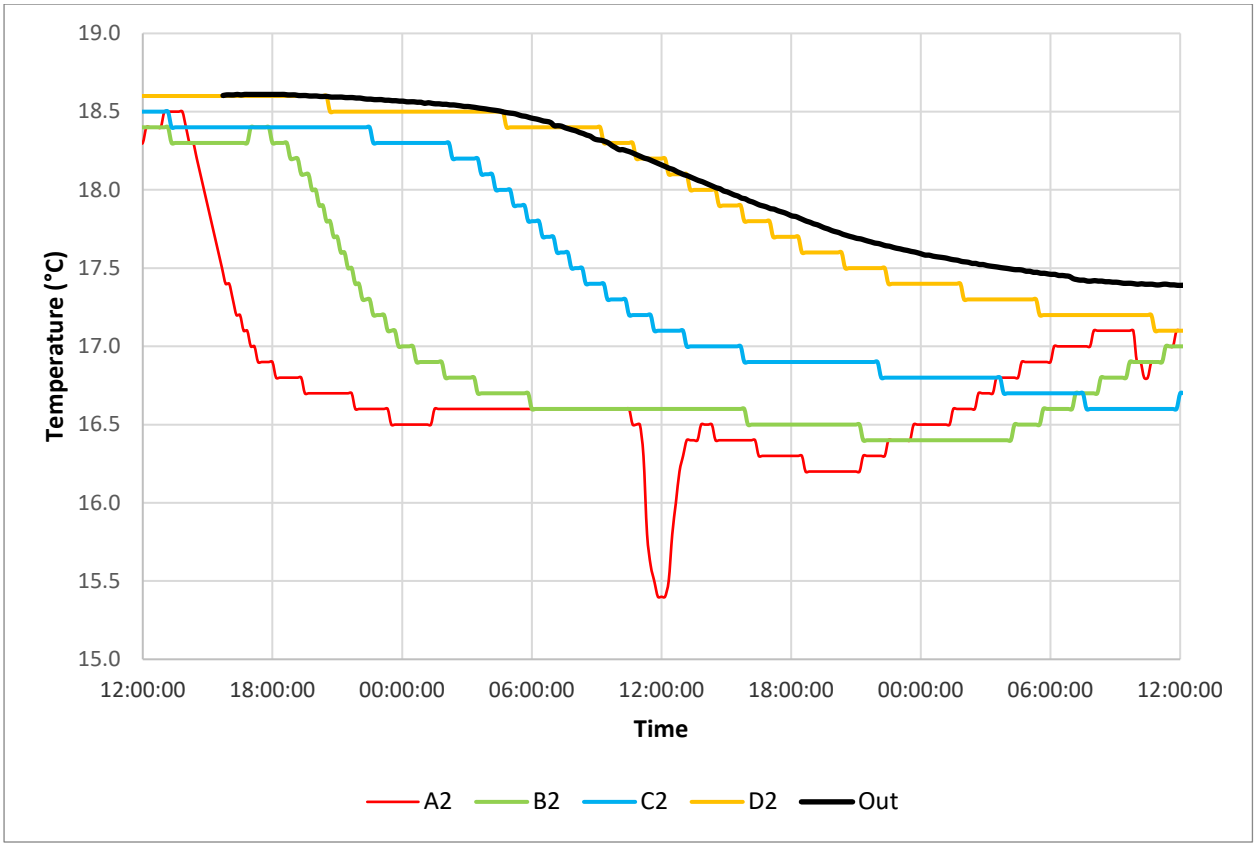

Figure 4. 7: Observed temperatures in each monitoring point versus time.

The variation of temperature with respect to time can be noticed from figure 4.7. It can be observed in the curve A2, a sudden decrease in the temperature due to the endothermic reaction induced by the dissolution of NaCl which has a slightly positive enthalpy at standard conditions. The change was due to the removal and reinsertion of the salt crystal from the injection point. The average velocity was measured by noticing the transfer of temperature over time from one curve to the other. For each curve the time and temperature were recorded at inflection point (center of the heat pulse). To find out the velocity, known distance was divided by the time recorded. The results are shown in table 4.5.

Table 4. 5: Average velocity measured from different measuring points taken at the (temperature (inflection point).

Average Velocity from Temperature (inflection point)				
Name	Distance	Time	Avg Velocity (m/hr.)	Avg Velocity (m/d)
A2-B2	0.5	6.0	0.1	2.0
A2-C2	1.5	16.3	0.1	2.2
A2-D2	3.0	26.0	0.1	2.8
A2-Out	3.5	29.3	0.1	2.9
B2-C2	1.0	11.3	0.1	2.1
B2-D2	2.5	21.0	0.1	2.9
B2-Out	3.0	24.3	0.1	3.0
C2-D2	1.5	9.7	0.2	3.7
C2-Out	2.0	13.0	0.2	3.7
D2-Out	0.5	3.3	0.2	3.6

The EC was the other main parameter recorded. While measuring the velocity from the EC, there were several gaussian peaks in the curve which corresponds to the insertion, removal, and reinsertion of the salt crystal. Due to the reason, the transfer of EC over time was performed for each gaussian breakthrough curves (BTC). From figure 4.8, it can be seen a sudden increase in the concentration of A2 which is the insertion of salt crystal and then it became steady till the removal of the salt crystal. For each insertion, removal and reinsertion of the salt crystal, the same trend is followed in all the curves.

By looking at the curve B2, it can be noticed that three gaussian BTC are formed, but the curve is not steady. The curve reaches the peak value and then instead of becoming steady, the EC again decreases. This turbulence can be due to the injection of the salt crystal in A2, B2 being close to the source (near source). In this case, the velocity for all the three BTC was measured by noticing the time at the peak of the curve instead of the inflection point.

At Point C2, after reaching breakthrough, the curve becomes steady unless the salt is removed. Two values of the velocities were taken by noticing the values at inflection point. At point D2, only on BTC was noticed, and velocity was found with respect to that curve. For the probes place outside of the tank, the velocities were calculated for each point. The results for all the points are listed in table 4.6.

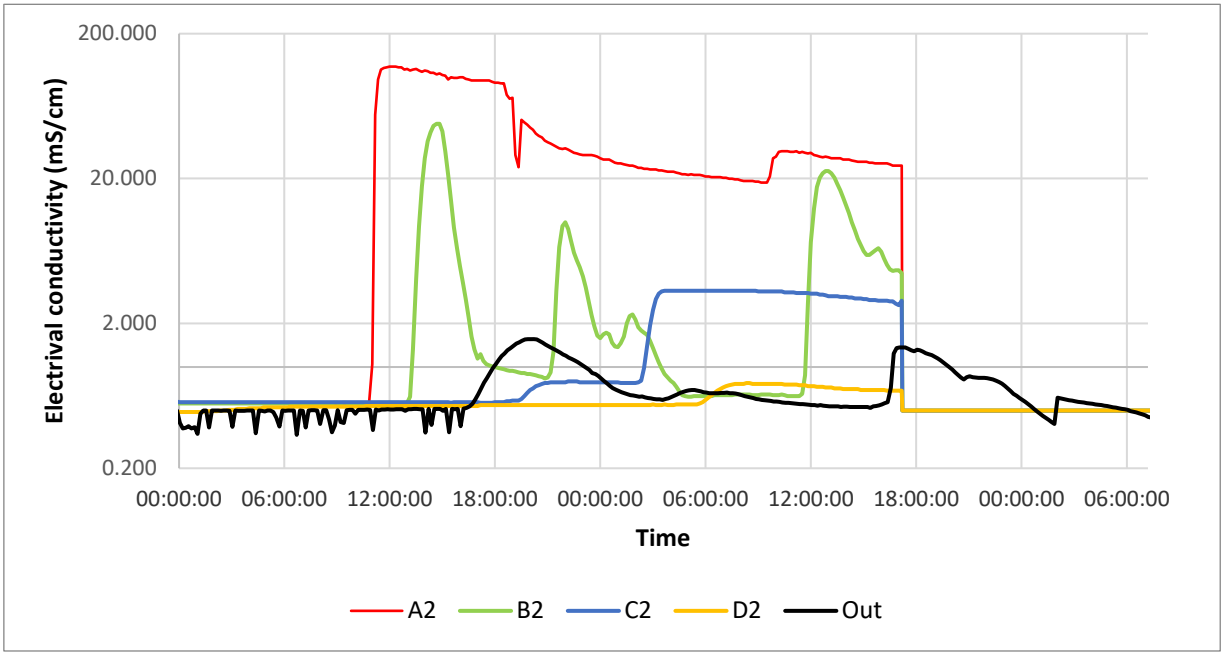

Figure 4. 8: Observed electrical conductivity in each monitoring point versus time

Table 4. 6: Average velocity calculated from the inflection points and peak of Gaussian BTC of EC among monitored points.

Average velocity from the EC				
Name	Distance	Time	Avg Velocity (m/hr)	Avg Velocity (m/d)
A2-B2 (insertion of salt)	0.5	2.5	0.2	4.8
A2-B2 (Removal of salt)	0.5	2.0	0.3	6.0
A2-B2 (Reinsertion of salt)	0.5	2.5	0.2	4.8
A2-C2 (insertion of salt)	1.5	9.0	0.2	4.0
A2-C2 (Removal of salt)	1.5	7.5	0.2	4.8
A2-D2	3.0	20.0	0.2	3.6

A2-Out (Insertion of Salt	3.5	8.0	0.4	10.5
A2-Out (Removal of salt)	3.5	9.0	0.4	9.3
A2-Out (Reinsertion of Salt)	3.5	8.0	0.4	10.5
B2-C2 (Insertion of Salt)	1.0	6.0	0.2	4.0
B2-C2 (Removal of Salt)	1.0	7.0	0.1	3.4
B2-D2	2.5	17.0	0.1	3.5
B2-Out (Insertion of Salt	3.0	5.0	0.6	14.4
B2-Out (Removal of salt)	3.0	7.0	0.4	10.3
B2-Out (Reinsertion of Salt)	3.0	5.0	0.6	14.4
C2-D2	1.5	11.0	0.1	3.3
C2- out (insertion of salt)	2.0	-1.0	-2.0	-48.0
C2-out (Removal of salt)	2.0	1.0	2.0	48.0
D2-Out	0.5	-16.0	0.0	-0.8

The seepage velocities calculated in Table 4.2, using the Darcy law was much higher than the one calculated from the temperature and EC curves. As by the formula it can be noticed that the Darcy velocities depend on the hydraulic conductivity, effective porosity and hydraulic gradient (k). Knowing the average hydraulic conductivity and the average porosity for the points, the only parameter which was different for each monitoring well was the hydraulic gradient and possibly local heterogeneities of hydraulic conductivity. The high value of velocities in the table 4.4, are due to high head gradient between the monitoring wells which in turn results in the high velocities.

The retardation factors were determined for the average velocities which are listed in table 4.7. As it can be noticed from table 4.6, the velocities calculated for EC of each monitoring well were more than one due to different BTC for same monitoring point. For this, average of the velocities was taken to calculate the retardation factors. Some of the values of the retardation factors were found to be above and others too low than the expected value of 1.99±0.06

(Alessandrino et al., 2022), this value was found using column experiments with the same material that fills the tank.

The reason for this can be the elevated heads gradient used in this experiment could have created zones of focusing flow bypassing the monitoring wells that have slotted pipes with 0.4 mm apertures, which have an equivalent hydraulic conductivity slightly lower than the one observed in the tank and thus could have been bypassed by the tracer. Or the removal of the injected salt crystal from the well to check the availability of salt. Another reason can be that the density of water was changed by the addition of the salt source which changes the flow of water, while in tracers test it is important to not perturb the properties of water that in turn affect the flow field.

Table 4. 7: Retardation factor calculated by velocity from EC over velocity from temperature.

Retardation Factor			
Name	Avg velocity from T (m/d)	Avg velocity from EC (m/d)	Retardation factor (-)
A2-B2	2.00	5.20	2.60
A2-C2	2.20	4.40	2.00
A2-D2	2.77	3.89	1.41
A2-Out	2.86	10.11	3.53
B2-C2	2.12	3.71	1.75
B2-D2	2.86	3.87	1.35
B2-Out	2.96	13.03	4.40
C2-D2	3.73	3.79	1.02
C2-Out	3.69	0.00	0.00
D2-Out	3.60	-0.65	-0.18

4.3.2 Tank experiment with PLA osmotic exchange bags

The experiment was performed in the same tank used in the experiment. 50 g of NaCl was added to the PLA bag. The PLA bag was introduced to the monitoring well A2. The flow was provided to the tank using a constant head reservoir (60 cm) by opening the inlet valve. Four

probes were placed in the monitoring well A2, B2, C2 and D2. A 5TE® Meter probe (Meter Environment, Pullman, WA, USA) was used in vadose zone for monitoring the volumetric water content (VWC), temperature, soil bulk EC. All the probes were connected to the meter data logger (ECH2O) having interval of recording as 10 minutes. At the outlet of the tank portable diver data logger was placed to record the variation of EC at interval of 10 minutes.

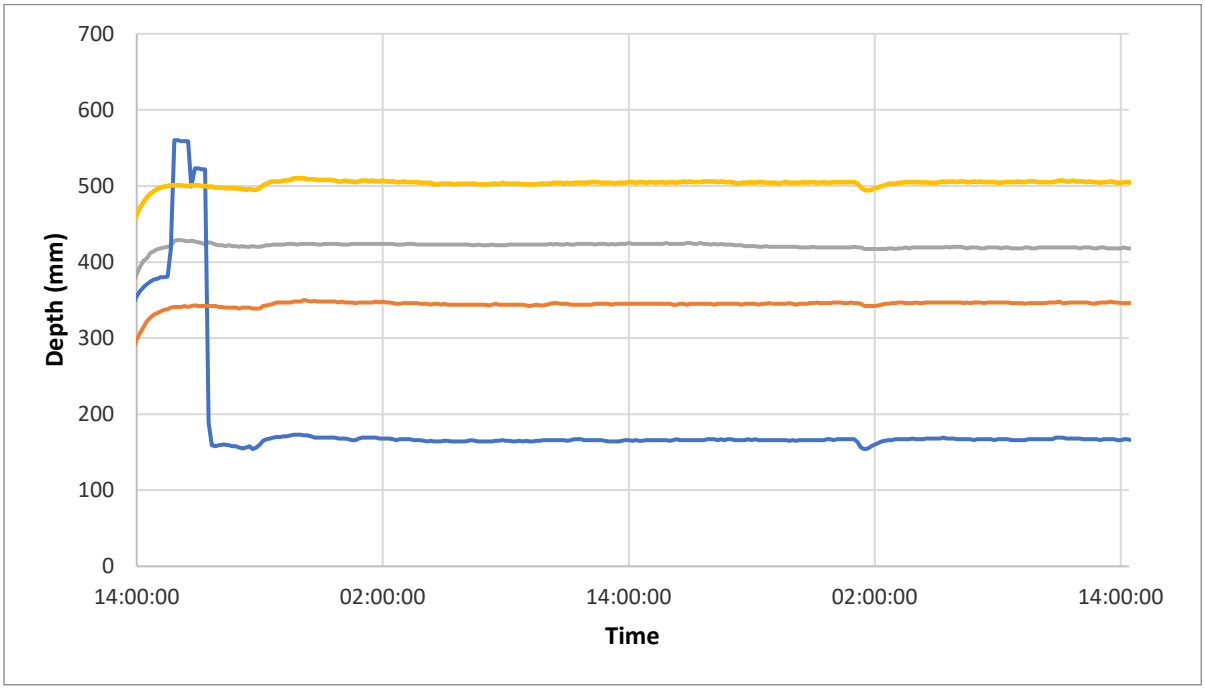

Figure 4. 9: Water level for the points A2, B2, C2 and D2.

The experiment was started on 24th May 2022 (12:00) and continued till 27th May 2022 (14:30). The hydraulic head in the tank is shown in the figure 4.9. The depth of all the probes is steady and they follow the same trend. At point A2, there is sudden decrease in the depth which was due to changing the depth of the probe in the monitoring well. After 1.5 hours the flow become steady and no variation in the depth were noticed.

The EC was the other main parameter recorded. Figure 4.10 shows the time variation of EC, the flow velocities were calculated by dividing the known horizontal distance between the monitoring well by the time taken to reach the inflection point of the curve. The EC in monitoring well reaches at its maximum point at 19:10, it decreases rapidly instead of becoming steady, which was due to relocation the probe in the monitoring well and disturbance of the salt source. The EC values of the C2 are not shown due to probe malfunction. While in B2 the NaCl plume was not constant, resembling the input function, while in D2 the EC remained stable probably because of a low permeability lens that trapped the saline plume. The velocities obtained from the variation of EC are listed in table 4.8.

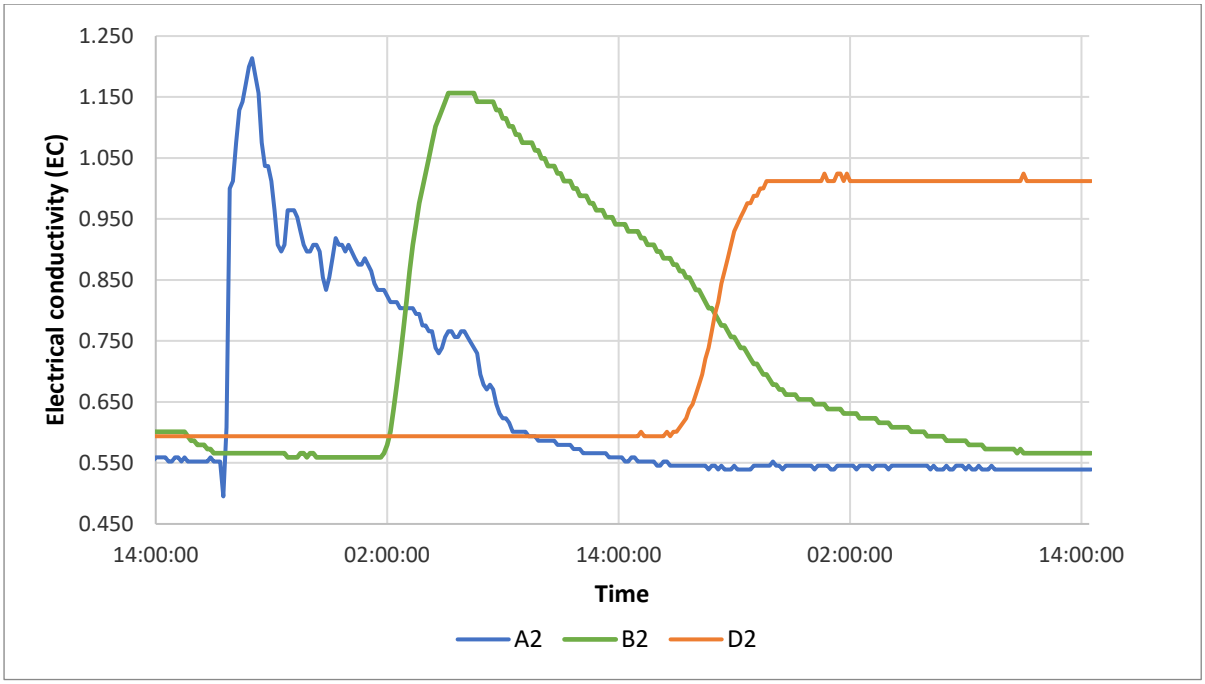

Figure 4. 10: Observed EC in each monitoring point versus time

Table 4. 8: Average velocity calculated from the inflection points of EC among the monitored points.

Average Velocity from EC				
Name	Distance	Time	Avg Velocity (m/hr)	Avg Velocity (m/d)
A2-B2	0.5	10.2	0.05	1.18
A2-D2	3.0	26.7	0.11	2.70
B2-D2	2.5	16.5	0.15	3.64
Average Velocity			2.50	

The velocity from point B2-D2 is the highest which can be noticed both graphically and in table, while the average velocity for the tank was calculated as 2.5 m/d.

Moreover, Darcy velocity and seepage velocity were also calculated knowing the values of the hydraulic head, porosity, and hydraulic conductivity of the tank. The values of hydraulic gradient were calculated by known value of the head and horizontal distance between monitoring points. The values are listed in table 4.9 below.

Table 4. 9: Hydraulic gradient between monitoring wells.

Hydraulic gradient				
Name	horizontal distance	Δh		Hydraulic gradient
		mm	m	
A2-B2	0.5	60	0.03	0.060
A2-C2	1.5	68	0.07	0.045
A2-D2	3	165	0.17	0.055
B2-C2	1	48	0.05	0.048
B2-D2	2.5	77	0.08	0.031
C2-D2	1.5	29	0.03	0.019

Furthermore, the average K value retrieved from the slug tests in each monitoring well is 34.5 m/d (Colombani et al., 2021), while the average n_e value is 0.2 (Alessandrino et al., 2022). The calculated Darcy and seepage velocity are listed in the table 4.10 below.

Table 4. 10: Calculated Darcy's and seepage velocities.

Monitoring wells	Hydraulic conductivity (m/d)	Porosity (m^3/m^3)	Head Gradient (m/m)	Darcy velocity (m/d)	Effective velocity (m/d)
A2-B2	34.5	0.2	0.06	6.07	10.35
A2-C2	34.5	0.2	0.045	3.13	7.76
A2-D2	34.5	0.2	0.055	1.90	9.49
B2-C2	34.5	0.2	0.048	1.66	8.28
B2-D2	34.5	0.2	0.031	1.06	5.31
C2-D2	34.5	0.2	0.019	0.67	3.34
Average velocity				7.42	

It can be noticed that the average effective velocity is about 7.42 m/d which means that the average retention time in the tank should be 0.54 days or 3 hours, moreove,r the effective velocity decreases towards the outflow of the tank due decrease in the hydraulic gradient.

The seepage velocities calculated in table 4.10 using the Darcy law is higher respect to the average velocity calculated from EC curves due to the elevated heterogeneities of the hydraulic conductivity field within the tank, for this reason a tracer test can be considered more accurate than a simple calculation via the Darcy law. Finally, this experiment highlighted that PLA bag have been well performed in maintaining low the salinity, thus avoiding changes in the groundwater density, which in turn could affect the flow field impairing the tracer test results.

Despite of this, the slow release of tracer is still not constant thus more effort must be paid to improve this technique.

4.3.3 Tank experiment with PLA osmotic exchange bags in a single well

To identify the vertical direction of the flow and the variation of EC at different depths in the tank, all the probes were transferred to a single monitoring well (D2). The probes were placed at the depths 39.6 cm, 29.5 cm, 16.3 cm, and 5.6 cm respectively. 55 gm of NaCl salt was added to PLA bag and it was introduced to the monitoring well in a way that it touched the water table. The flow was provided to the tank using a constant head reservoir (50 cm) by opening the inlet valve. At the outlet of the tank, the outflow tube was placed at 39 cm and portable diver data logger was placed to record the variation of EC at interval of 10 minutes.

The PLA bag with the salt was placed in the monitoring well at 10:08 in the morning and data was continuously recorded to get the breakthrough curves for EC. The data was checked continuously using EM 50 data logger. After obtaining the steady curves for EC, the salt source was removed at 15:04.

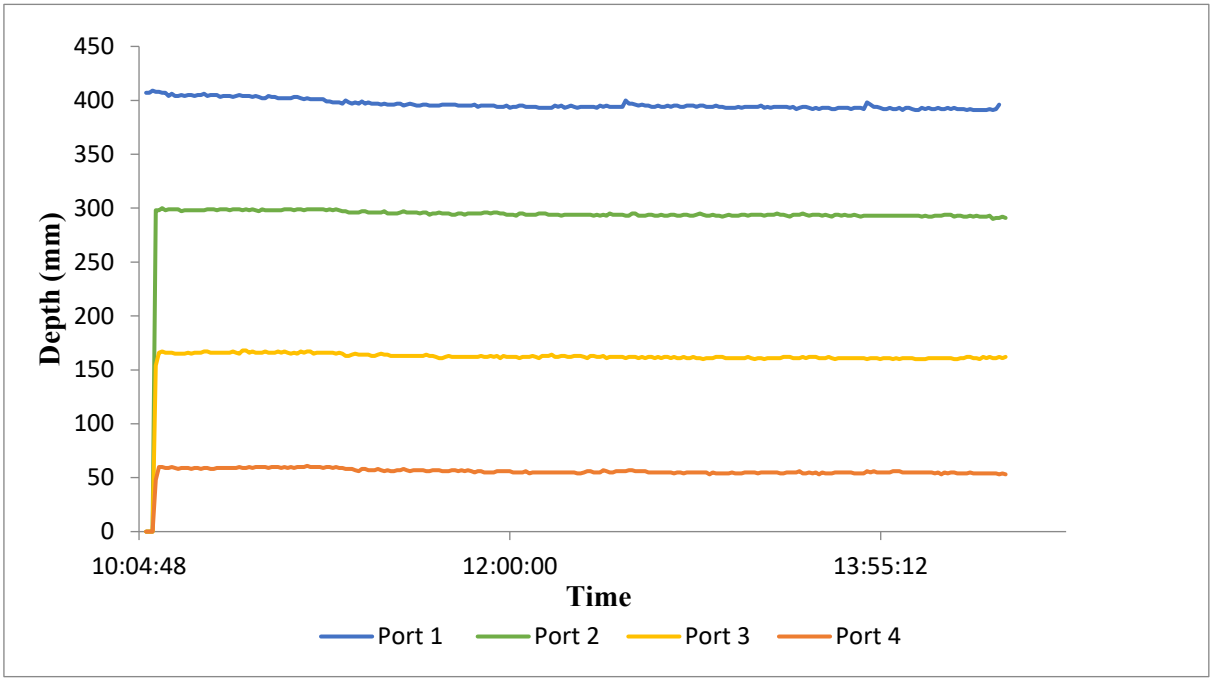

Figure 4. 11: Depth of the water recorded by the probes with variation of time.

The steadiness of flow and the hydraulic gradient are the important parameters in the tracer tests for providing constant boundary conditions. In figure 4.11, an increased jump can be noticed in the depth due to insertion of the exchange membrane which after a while becomes steady. Furthermore, it can also be noticed that the hydraulic gradient is steady and follow same

trends for all the probes, except there are instrumental fluctuations but it is acceptable as per accuracy of the probes used. Also, no major changes in the temperature were noticed during the experiment.

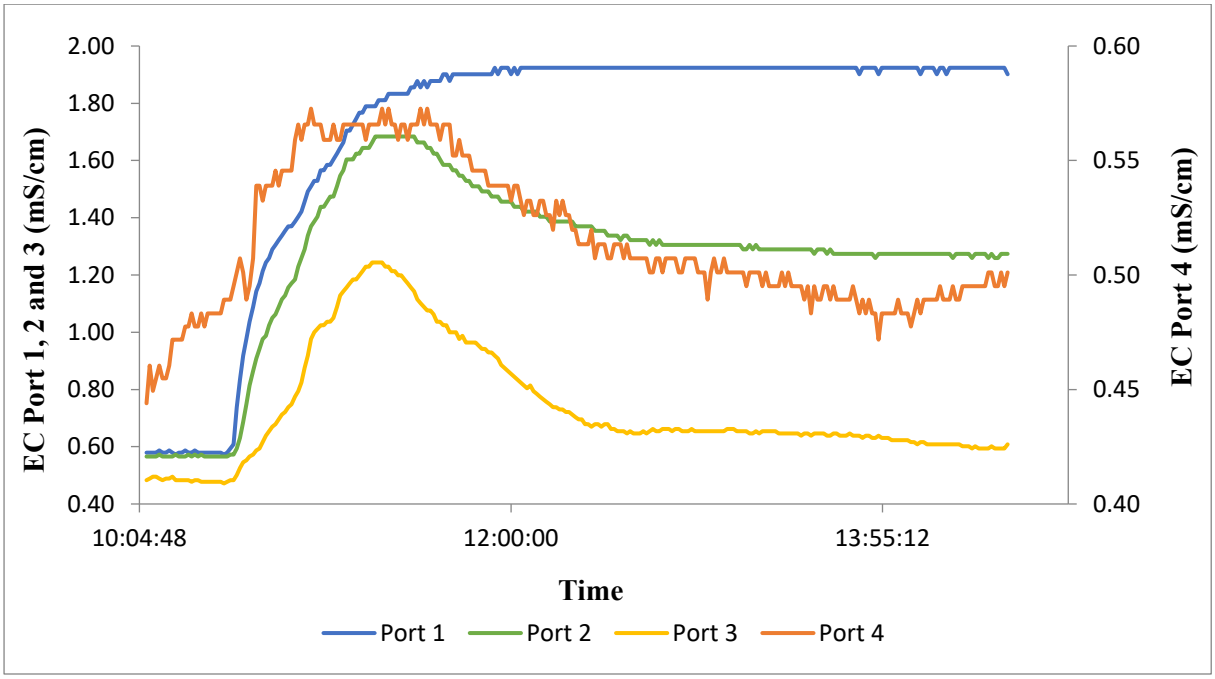

Figure 4. 12: Time variation of EC in a single monitoring well, note that Port 4 has a secondary Y axis (on the right).

Figure 4.12 shows the time variation of EC at different depths, it can be noticed that the EC increases faster in the port 4 being the shallowest one in the tank and the one located near to the PLA bag. Nevertheless, there is an evident vertical flow direction toward the bottom of the tank (Port 1) which showed the highest EC value (1.92 mS/cm). The flow showed a marked downward type of behaviour, in fact the salinity front moved downward increasing the EC in all the probes but then decreased to reach a steady value when the background flow reached equilibrium with the background flux, this was true for all the probes except for the deepest one (Port 1). This peculiar behaviour could be explained by a horizontal flow component in the well that further displaced the EC breakthrough in the upper probes; while in the lower one the EC did not show any decrease, thus suggesting vertical flow only. To calculate the flow velocity, the depth of the probe was divided by the time to reach half of the breakthrough curve peak for Port 4, 3 and 2 and at the midpoint among the lower and higher EC value in Port 1.

The velocity was calculated for each probe and finally the average velocity for the flow was obtained in the vertical direction. The results are listed in the table 4.12 below.

Table 4. 11: Calculation of the average velocity of the flow from the time taken to achieve breakthrough curves.

Name	Distance (cm)	Time (hr)	Avg Velocity (cm/hr)	Avg Velocity (m/d)
P1	39.6	1.56	25.3	6.1
P2	29.5	1.23	24.0	5.8
P3	16.3	1.13	14.2	3.4
P4	5.6	0.78	7.2	1.7

The values listed in the table verify the downward flow direction in the tank, with increasing values towards the bottom of the tank. The low velocity of the flow at the upper probe can be results of the recirculation of the flow. Furthermore, the values of EC were also checked in the porewater of tank by the micro sampling ports which are placed outside the piezometer, the results are displayed in the table below.

Table 4. 12: EC values obtained from actual aquifers in the tank

EC in porewater outside the D2 well	
Name	EC (mS/cm)
P1 (55 cm)	-
P2 (45 cm)	0.591
P3 (35 cm)	0.726
P4 (25 cm)	0.620
P5 (15 cm)	0.552
P6 (5 cm)	0.482

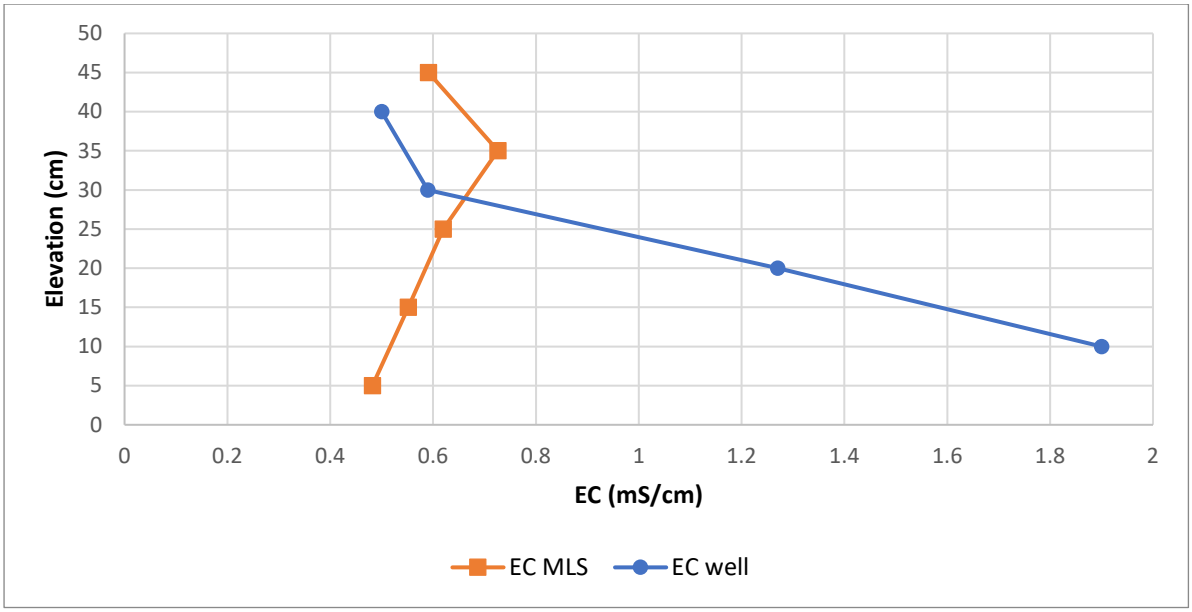

Figure 4. 13: Comparison of EC between the MLS outside D2 and in monitoring well D2.

The micro sampling ports were installed at every 10 cm vertical distance from each other in the tank to capture vertical salinity variations. To check the EC in the porewater, at least 20 ml water sample was pumped from each port and the values were recorded. As listed in the table 4.13, the extraction of porewater was not possible even using peristaltic pump from the Port 1 due to some blockage. Due to low hydraulic conductivity in the tank near the P2 port, the use of peristatic pump was the only possibility to extract the water sample. The extraction from the remaining ports were easy due to their elevated hydraulic conductivities.

The variation of EC in the tank outside the well D2 confirmed that a horizontal component was present in the upper part of the tank while no horizontal flow was present at the tank's botto

Conclusions

Groundwater degradation is an alarming evidence of climate change, and its early identification is the aim of many research studies. Advancement in the tracer techniques has experienced improvements in the last decades to provide valuable information at early stages about groundwater degradation and the sources and pathway of contamination. Following the rationale of diminishing time efforts and costs of monitoring tracer tests, a cost-effective technique was developed to produce a pseudo-constant source of tracer that could be much more easily tracked and monitored respect to instantaneous injections. To this purpose a low-cost ion exchange membrane was tested, namely using PLA bags. Tests included batch experiments, one-dimensional column and three-dimensional tank experiments in controlled laboratory conditions at SIMAU department of "Università Politecnica delle Marche".

The results obtained from the batch experiments showed that biodegradable PLA bags were able to act as a low efficiency exchange membrane for the slow release of NaCl in groundwater. Moreover, it provided a base for further lab experiments using it as slow-release tracer source with a well-known MLR. In fact, the results obtained from one-dimensional column experiments showed PLA bags can be considered a good candidate to be used as an exchange membrane due to its low MLR efficiency for the NaCl release. This because in tracer testing techniques the priority is to choose a membrane (acting as a pseudo-constant source) which can release the solute at a low rate without changing the density and viscosity of water. The results highlighted that NaCl MLR was increasing logarithmically with the groundwater specific discharge, thus high NaCl concentrations are to be expected in fast flow fields.

Finally, a series of three-dimensional tank (multilevel monitoring wells and single monitoring well) experiments highlighted that using large NaCl crystals encapsulated in 50 μm mesh bags did provide a constant source of tracer but the concentration highly exceeded the threshold to trigger density dependent flow, with EC values up to 100 mS/cm in the source well. While using a PLA bag the maximum EC value was up to 1.25 mS/cm in the source well and was still distinguishable at 3 m distance. In the single well monitoring experiment, the EC increased faster in the shallow portion of the tank near to the injected source and an evident vertical flow direction toward the bottom was detected only within the monitoring well that acted as a preferential pathway. For all probes except the deepest, a marked downward type of behaviour of the flow was noticed, in fact the salinity front moved downward increasing the EC in all the probes but then decreased to reach a steady value when the background flow reached equilibrium with the background flux. The variation of EC in the tank outside the well

confirmed that a horizontal component was present in the upper part of the tank while no horizontal flow was present at the tank's bottom. Thus, even used as single well tracer test this low-cost technique provided reliable results.

The findings from all experiments highlighted that PLA bag have well performed in maintaining low the EC and thus the salinity, avoiding changes in groundwater density, which in turn could affect the flow field impairing the tracer test results. The continuous EC monitoring allowed to capture the tracer breakthrough and to estimate the mean flow velocities and this may be relevant to understand when and where the plume is fully developed to make a single field campaign instead of multiple ones, thus saving time and money. Moreover, the PLA bag was kept in contact with a solution more than a month to check the degradation or damage to the bag, but it was found to be in good condition, and this make it a good candidate to be employed safely for at least a week as continuous source of tracer in a well. Further development of this technique will be its employment in field experiments to better understand the efficiency and accuracy of PLA as exchange membrane in the relevant environment.

References

Alessandrino, L., Eusebi, A. L., Aschonitis, V., Mastrocicco, M., & Colombani, N. (2022). Variation of the hydraulic properties in sandy soils induced by the addition of graphene and classical soil improvers. Journal of Hydrology, 128256. https://doi.org/10.1016/j.jhydrol.2022.128256

Aquilanti, L., Clementi, F., Landolfo, S., Nanni, T., Palpacelli, S., & Tazioli, A. (2013). A DNA tracer used in column tests for hydrogeology applications. Environmental earth sciences, 70(7), 3143-3154. https://doi.org/10.1007/s12665-013-2379-y

Boggs, J. M., Young, S. C., Beard, L. M., Gelhar, L. W., Rehfeldt, K. R., and Adams, E. E. (1992). Field study of dispersion in a heterogeneous aquifer: 1. Overview and site description. Water Resour. Res. 28, 3281–3291. https://doi.org/10.1029/92WR01756

Brennwald, M. S., Peel, M., Blanc, T., Tomonaga, Y., Kipfer, R., Brunner, P., & Hunkeler, D. (2022). New Experimental Tools to Use Noble Gases as Artificial Tracers for Groundwater Flow. Frontiers in Water, 4. https://doi.org/10.3389/frwa.2022.925294

Chen, X., Murakami, H., Hahn, M. S., Hammond, G. E., Rockhold, M. L., Zachara, J. M., and Rubin, Y. (2012), Three-dimensional Bayesian geostatistical aquifer characterization at the Hanford 300 Area using tracer test data, Water Resour. Res., 48, W06501, https://doi.org/10.1029/2011WR010675

Colombani, N., Fronzi, D., Palpacelli, S., Gaiolini, M., Gervasio, M. P., Marcellini, M., Mastrocicco, M., Tazioli, A. (2021). Modelling Shallow Groundwater Evaporation Rates from a Large Tank Experiment. Water Resources Management, 35(10), 3339-3354. https://doi.org/10.1007/s11269-021-02896-2

Colombani, N., Giambastiani, B. M. S., & Mastrocicco, M. (2015). Combined use of heat and saline tracer to estimate aquifer properties in a forced gradient test. Journal of Hydrology, 525, 650-657. https://doi.org/10.1016/j.jhydrol.2015.04.026

Cook, P. G. (2015). The Role of Tracers in Hydrogeology. In Groundwater (Vol. 53, Issue S1, pp. 1–2). https://doi.org/10.1111/gwat.12327

Cuevas, J., Daliakopoulos, I. N., del Moral, F., Hueso, J. J., Tsanis, I. K. (2019). A review of soil-improving cropping systems for soil salinization. Agronomy, 9(6), 295. https://doi.org/10.3390/agronomy9060295

Divine, C. E., & McDonnell, J. J. (2005). The future of applied tracers in hydrogeology. Hydrogeology Journal, 13(1), 255–258. https://doi.org/10.1007/s10040-004-0416-3

Eamus, D., Zolfaghar, S., Villalobos-Vega, R., Cleverly, J., & Huete, A. (2015). Groundwater-dependent ecosystems: recent insights from satellite and field-based studies. Hydrology and Earth System Sciences, 19(10), 4229-4256. https://doi.org/10.5194/hess-19-4229-2015

FAO (2021), The State of the World's Land and Water Resources for Food and Agriculture – Systems at breaking point. Synthesis report 2021. Rome. https://doi.org/10.4060/cb7654en

Garabedian, S. P., LeBlanc, D. R., Gelhar, L. W., & Celia, M. A. (1991). Large-scale natural gradient tracer test in sand and gravel, Cape Cod, Massachusetts: 2. Analysis of spatial moments for a nonreactive tracer. Water Resources Research, 27(5), 911-924. https://doi.org/10.1029/91WR00242

Garcia-Vasquez, W., Ghalloussi, R., Dammak, L., Larchet, C., Nikonenko, V., & Grande, D. (2014). Structure and properties of heterogeneous and homogeneous ion-exchange membranes subjected to ageing in sodium hypochlorite. Journal of Membrane Science, 452, 104-116. https://doi.org/10.1016/j.memsci.2013.10.035

Kalbus E., Reinstorf F., Schirmer M. (2006). Measuring methods for groundwater – surface water interactions: a review. Hydrol. Earth Syst. Sci., 10, 873–887. https://doi.org/10.5194/hess-10-873-2006

Kløve, B., Ala-Aho, P., Bertrand, G., Boukalova, Z., Ertürk, A., Goldscheider, N., ... & Widerlund, A. (2011). Groundwater dependent ecosystems. Part I: Hydroecological status and trends. Environmental Science & Policy, 14(7), 770-781. https://doi.org/10.1016/j.envsci.2011.04.002

Mastrocicco, M., Colombani, N. (2021). The issue of groundwater salinization in coastal areas of the mediterranean region: A review. Water, 13(1), 90. https://doi.org/10.3390/w13010090

Moeck, C., Radny, D., Popp, A., Brennwald, M., Stoll, S., Auckenthaler, A., ... & Schirmer, M. (2017). Characterization of a managed aquifer recharge system using multiple tracers. Science of the Total Environment, 609, 701-714. https://doi.org/10.1016/j.scitotenv.2017.07.211

National Geographic Society (2022), Groundwater. National Geographic. https://education.nationalgeographic.org/resource/groundwater

NGWA – The Groundwater Association (2022), Facts about global groundwater usage. https://www.ngwa.org/what-is-groundwater/About-groundwater/facts-about-global-groundwater-usage

Pang, L., Abeysekera, G., Hanning, K., Premaratne, A., Robson, B., Abraham, P., ... & Billington, C. (2020). Water tracking in surface water, groundwater and soils using free and alginate-chitosan encapsulated synthetic DNA tracers. Water Research, 184, 116192. https://doi.org/10.1016/j.watres.2020.116192

Prasad N. B. (2002), Groundwater hydrogeology. https://www.researchgate.net/publication/317328777_Groundwater_Hydrology

Ptak, T., & Teutsch, G. (1994). Forced and natural gradient tracer tests in a highly heterogeneous porous aquifer: Instrumentation and measurements. Journal of Hydrology, 159(1-4), 79-104. https://doi.org/10.1016/0022-1694(94)90250-X

Ptak, T., Piepenbrink, M., & Martac, E. (2004). Tracer tests for the investigation of heterogeneous porous media and stochastic modelling of flow and transport - A review of some recent developments. Journal of Hydrology, 294(1–3), 122–163. https://doi.org/10.1016/j.jhydrol.2004.01.020

Rhoades, J. D., Kandiah, A., Mashali, A. M. (1992). The use of saline waters for crop production-FAO irrigation and drainage paper 48. FAO, Rome, 133.

Sudicky, E. A. (1986). A natural gradient experiment on solute transport in a sand aquifer: Spatial variability of hydraulic conductivity and its role in the dispersion process. Water resources research, 22(13), 2069-2082. https://doi.org/10.1029/WR022i013p02069

USGS – science for a changing world (2018), Nitrogen and Water. https://www.usgs.gov/special-topics/water-science-school/science/nitrogen-and-water

USGS – science for a changing world (2019), Nutrients and eutrophication. https://www.usgs.gov/mission-areas/water-resources/science/nutrients-and-eutrophication#overview

van der Gun, J. (2021). Groundwater resources sustainability. In Global groundwater (pp. 331-345). Elsevier. https://doi.org/10.1186/s12302-022-00646-8

van Weert F., van der Gun J., Reckman J. (2009), Global Overview of Saline Groundwater Occurrence and Genesis, pp. 5 et seq., https://www.un-igrac.org/sites/default/files/resources/files/Global%20Overview%20of%20Saline%20Groundwater%20Occurences%20and%20Genesis.pdf

Verreydt, G., Bronders, J., Van Keer, I., Diels, L., Vanderauwera, P. (2010). Passive samplers for monitoring VOCs in groundwater and the prospects related to mass flux measurements. Groundwater Monitoring & Remediation, 30(2), 114-126. https://doi.org/10.1111/j.1745-6592.2010.01281.x

Ward M. H., Jones R. R., Brender J. D., de Kok T. M., Weyer P. J., Nolan B. T., Villanueva C. M., van Breda S. G. (2018), Drinking Water Nitrate and Human Health: An Updated Review. Int J Environ Res Public Health, 15(7):1557. doi:10.3390/ijerph15071557

Zheng, C., Bianchi, M., & Gorelick, S. M. (2011). Lessons learned from 25 years of research at the MADE site. Groundwater, 49(5), 649-662. https://doi.org/10.1111/j.1745-6584.2010.00753.x